

# Advanced Complex Hydrides: Development and Fundamental Studies of Promising New Hydrogen Storage Materials

Craig M. Jensen  
Dept. of Chemistry  
University of Hawaii

# DOE FreedomCar Technical Targets On-Board Hydrogen Storage System (300 mile range - 5.6 kg H<sub>2</sub>)



Property	Units	Target
Hydrogen Density (gravimetric)	wt.% H	6
Energy Efficiency	%	97
Energy Density (volumetric)	W-h/L	1100
Hydrogen Density (volumetric)	kg H <sub>2</sub> /m <sup>3</sup>	33
Specific Energy	W-h/kg	2000
Cost	\$/kW-h	5
	(\$/kg H <sub>2</sub> )	(167)
Operating Temperature	°C	-40 - +50
Start-Up Time to Full Flow	sec	15
Hydrogen Loss	scc/hr/L	1.0
Cycle Life	cycles	500
Refueling Time	min	<5
Recoverable Usable Amount	%	90

# Capacity and Cost Comparisons of Representative Hydrides - Class by Class

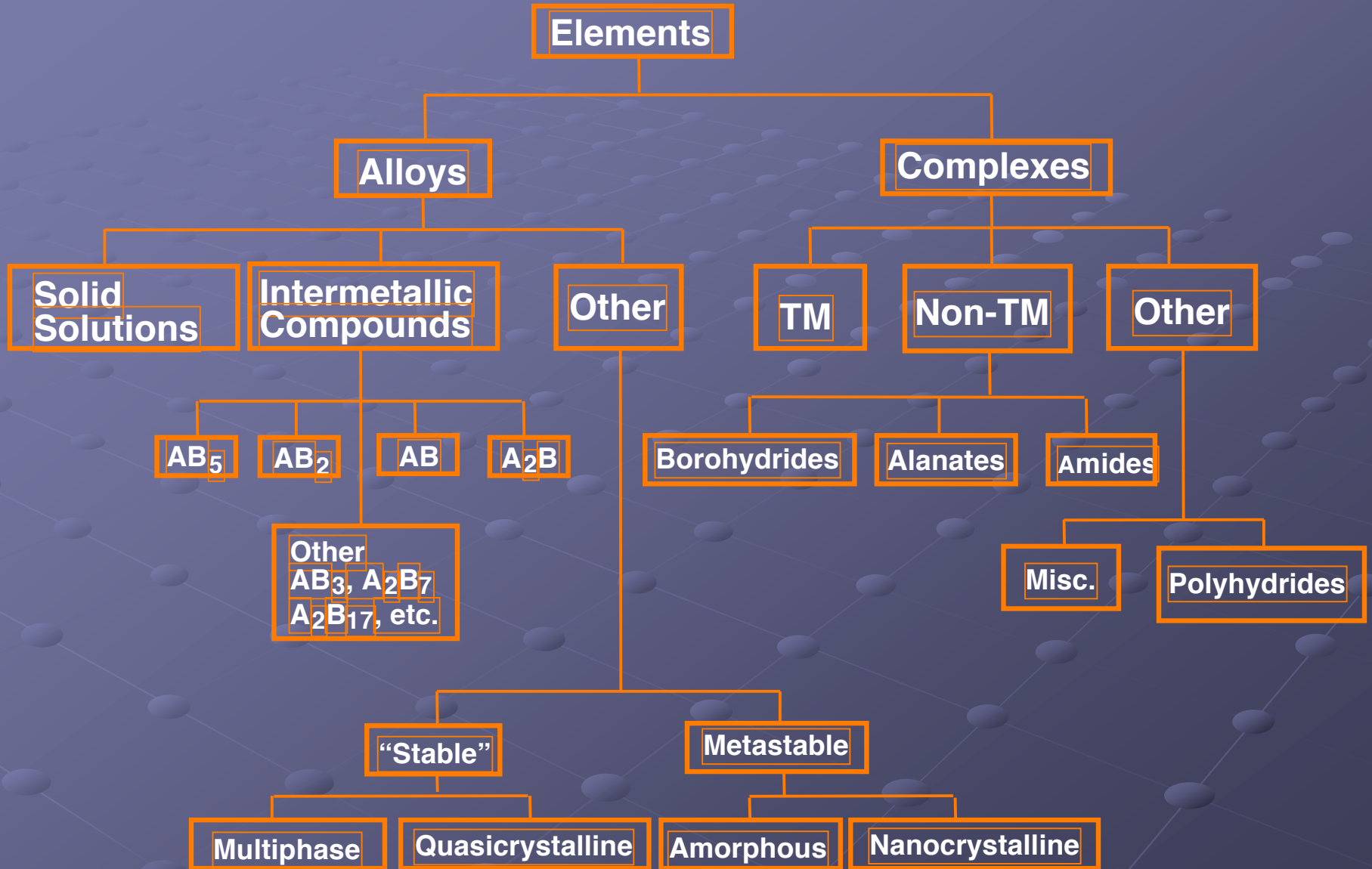
Composition	(H-Capacity) <sub>rev</sub>			T for 1 atm, °C	Alloy RMC**	
	$\Delta H/M$	$\Delta wt, \%$	$\Delta N_H/V^*$		\$/kg	\$/g H
<b>AB<sub>5</sub>-Type</b>						
MmNi <sub>4.5</sub> Al <sub>0.5</sub>	0.58	0.83	3.5	-6	7.17	0.86
LaNi <sub>5</sub>	0.93	1.28	5.2	12	9.87	0.77
CaNi <sub>5</sub>	0.55	0.99	3.4	43	7.56	0.76
<b>AB<sub>2</sub>-Type</b>						
Ti <sub>0.98</sub> Zr <sub>0.02</sub> V <sub>0.43</sub> Fe <sub>0.09</sub> Cr <sub>0.05</sub> Mn <sub>1.5</sub>	0.7	1.3	3.8	-28	4.82	0.37
TiMn <sub>1.5</sub>	0.65	1.15	3.8	-21	4.99	0.44
<b>AB-Type</b>						
TiFe	0.79	1.5	5.0	-8	4.68	0.31
TiFe <sub>0.85</sub> Mn <sub>0.15</sub>	0.80	1.5	5.0	3	4.83	0.32
<b>SS-Type</b>						
(V <sub>0.9</sub> Ti <sub>0.1</sub> ) <sub>0.95</sub> Fe <sub>0.05</sub>	0.95	1.8	4.9	36	10.63	0.59
<b>A<sub>2</sub>B Type</b>						
Mg <sub>2</sub> Ni	1.23	3.3	5.2	255	6.26	0.19
<b>Mg</b>						
Mg (MgH <sub>2</sub> )	2.0	7.6	6.7	279	4.25	0.056
Mg (MgH <sub>1.3</sub> )***	1.3	5.0	4.4	279	10.00	0.20

\* In units of 10<sup>22</sup> H-atoms/crystal cm<sup>3</sup>

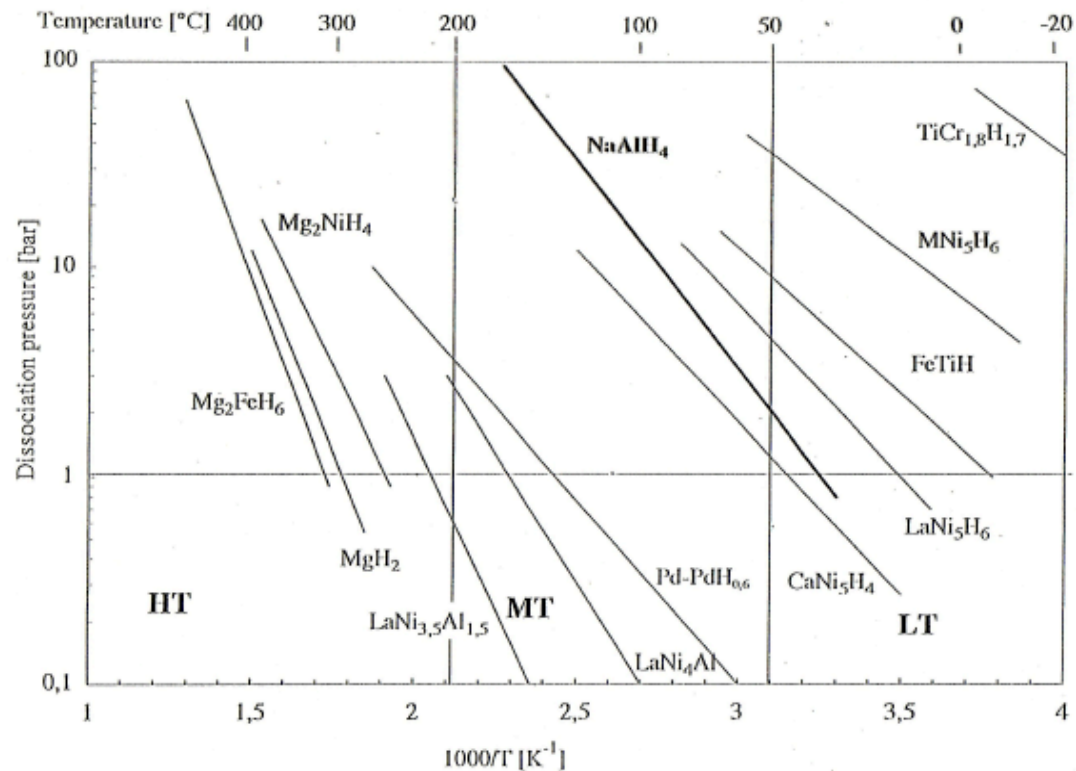
\*\* RMC = Raw Materials Cost; US\$/g H based on (H-Capacity)<sub>rev</sub>

\*\*\* Hydro-Québec high-energy ball-milled

# Metal Hydride Family Tree

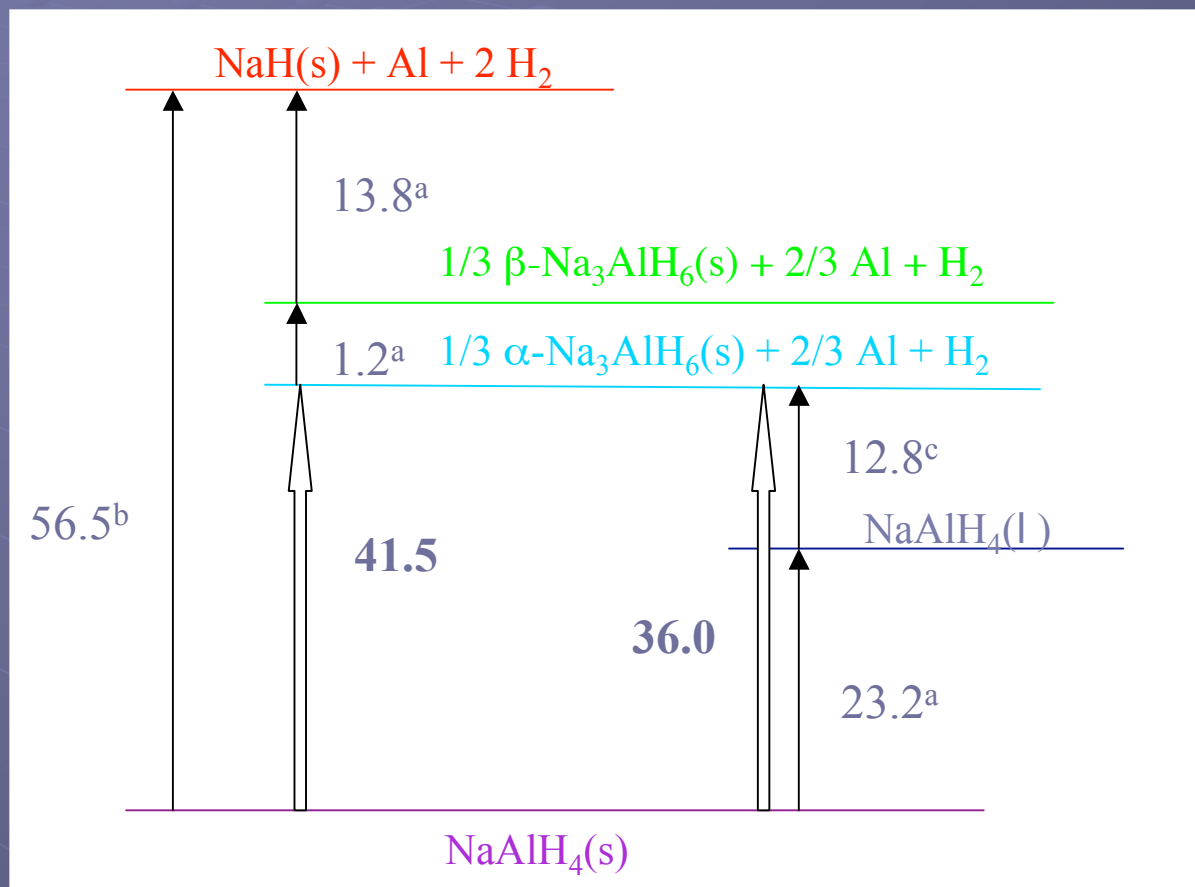


# Van't Hoff Plots of Various Metal Hydrides



B. Bogdanovic, R. A. Brand, A. Marjanovic, M. Schwickardi *J. Alloys and Comps.* 2000, 302, 36.

# Enthalpy Values (kJ) Associated with the Processes Occurring During the Dehydrogenation of One Mole of $\text{NaAlH}_4$

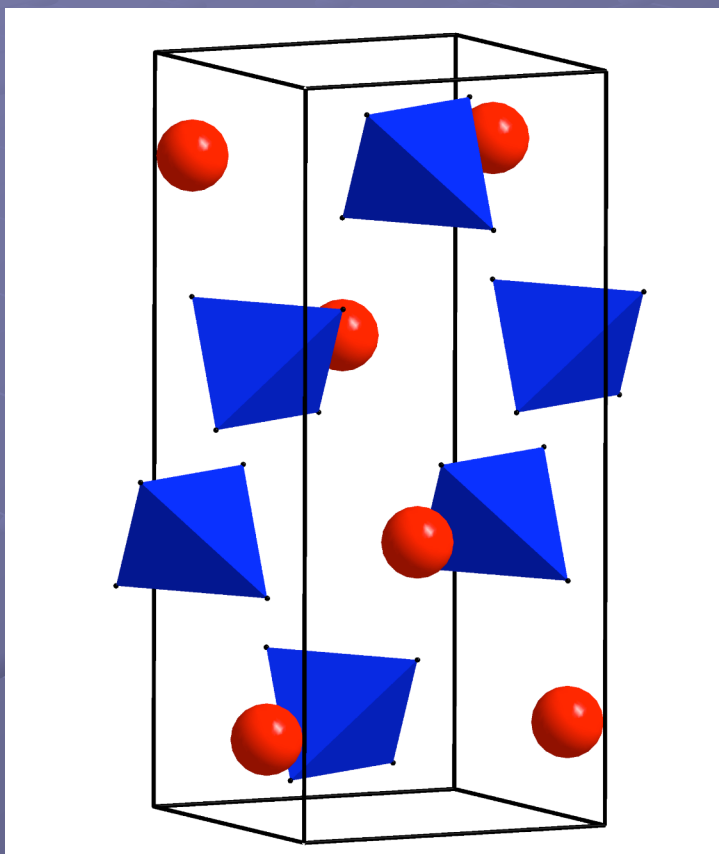


a) P. Claudy, B. Bonnetot, G. Chahine, J. M. Letoffe *Thermochim. Acta* 1980, 38, 75.

b) T. N. Dymova, S. I. Bakum *Russ. J. Inorg. Chem.* 1969, 14, 1683.

c) T. N. Dymova, Y. M. Dergachev, V. A. Sokolov, N. A. Grechanaya *Dokl. Akada. Nauk SSSR* 1975, 224, 591.

# Neutron Diffraction Structure Determination of NaAlD<sub>4</sub>



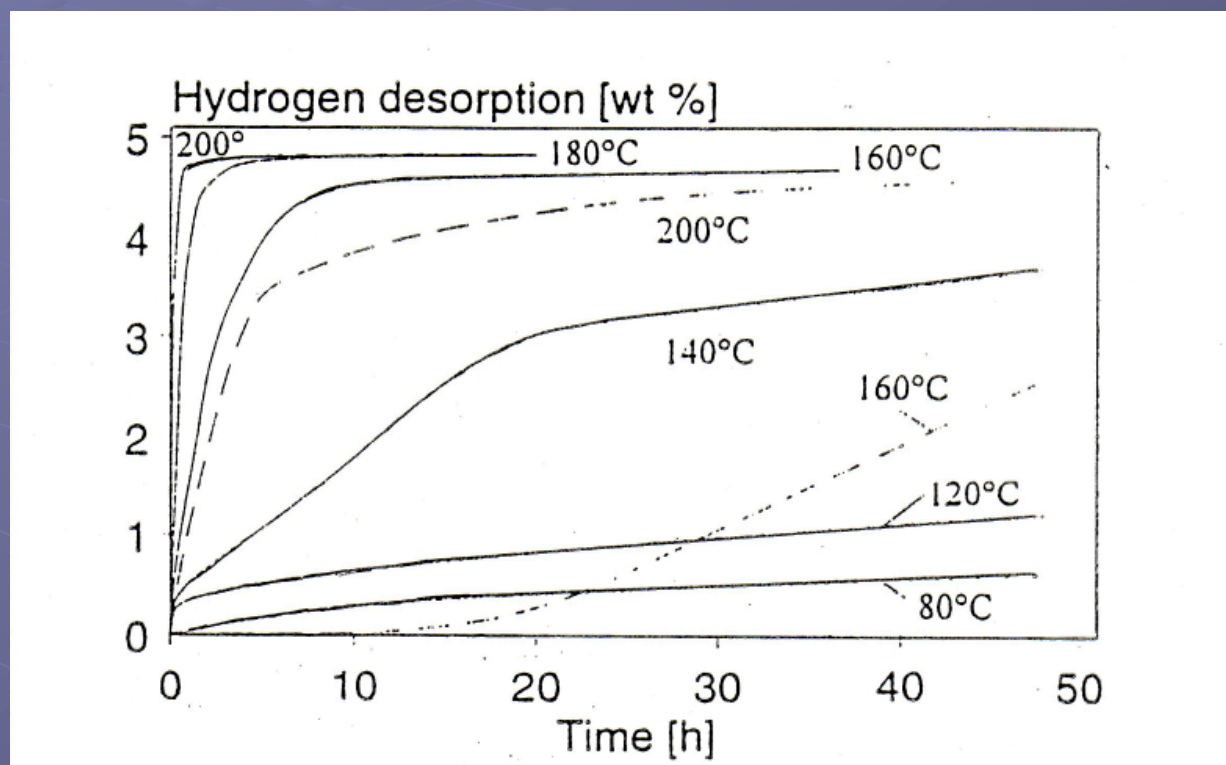
## Direct determination of hydrogen atom locations

Selected inter-atomic distances (pm) and angles (deg.) in the crystal structure of NaAlD<sub>4</sub> at 295 and 8 K. Estimated standard deviations in parentheses

Atoms	295 K	8 K
Al-D ( $\times 4$ )	162.6(2)	162.7(2)
Na-D ( $\times 4$ )	243.1(2)	240.3(2)
( $\times 4$ )	243.9(1)	240.5(2)
D-D ( $\times 2$ )	261.9(1)	262.0(1)
Na-Na ( $\times 4$ )	377.9(1)	373.7(1)
Al-Na ( $\times 4$ )	354.4(1)	352.1(1)
( $\times 4$ )	377.9(1)	373.7(1)
D-Al-D ( $\times 4$ )	107.32(1)	107.30(1)
( $\times 2$ )	113.86(1)	113.90(1)

B. Hauback, H. Brinks, C.M. Jensen, K. Murphy, A. Maeland *J. Alloys Compd.* 2003, 358, 142.

# Titanium Doping Enhances Dehydriding of $\text{NaAlH}_4$



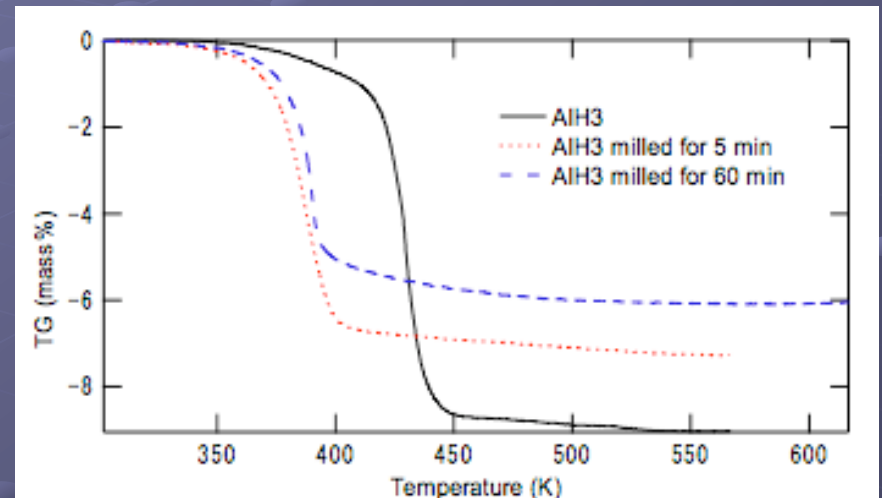
Progress of hydrogen desorption in the course of time at different temperatures for samples of  $\text{NaAlH}_4$ : undoped ----- and doped (2 mol%  $\text{Ti}(\text{OBu})_4$ ) —.

B. Bogdanovic and M. Schwickardi *J. Alloys and Comp.* **1997**, 253-254,1.

# Alane $\text{AlH}_3$



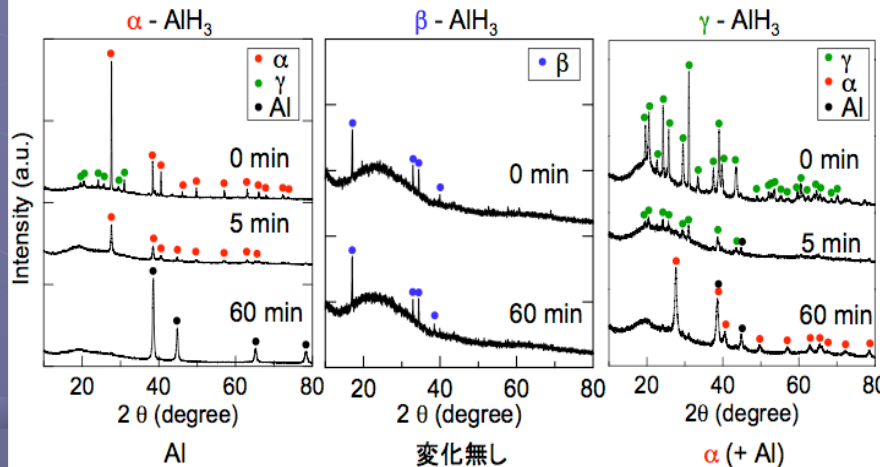
- 10 wt % available  $\text{H}_2$
- Known for 40 years<sup>1</sup>
- Controllable dehydrogenation at acceptable rates below 100 °C with additives<sup>2</sup> or if ball milled<sup>3</sup>
- Low ( $< 10$  kJ/mol)  $\Delta H_{\text{dehy}} \Rightarrow$  very high pressures for charging at ambient or higher temperatures



1. M. Appel, J.P. Frankel *J. Chem. Phys.* **1965**, *42*, 3984. F.M. Brower, N.E. Matzek, P.F. Reigler, H.W. Rinn, C.B. Roberts, D.L. Schmidt, J.A. Snover, K. Terada *J. Am. Chem. Soc.* **1976**, *98*, 2480.
2. G. Sandrock, J. Reilly, J. Graetz, W.-M. Zhou, J. Johnson, J. Wegrzy *Appl. Phys. A* **2005**, *80*, 687.
3. S. Orimo, Y. Nakamori, T. Kato, C. Brown, C.M. Jensen *Appl. Phys. A* **2006**, *83*, 5.

# Determination of the intrinsic and mechanically modified thermal stabilities of $\alpha$ , $\beta$ , and $\gamma$ alane (collaboration with Tohoku University)

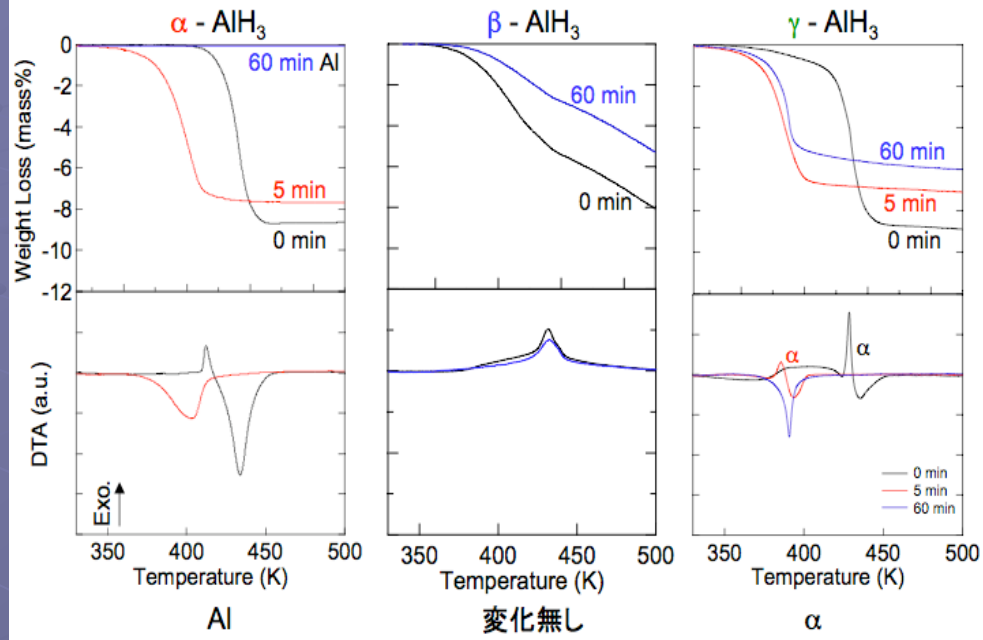
## X-ray diffraction



Profiles of the three phases of  $\text{AlH}_3$  before and after mechanical milling.

S. Orimo, Y. Nakamori, T. Kato, C. Brown, C.M. Jensen Appl. Physics **2006** 117, 27.

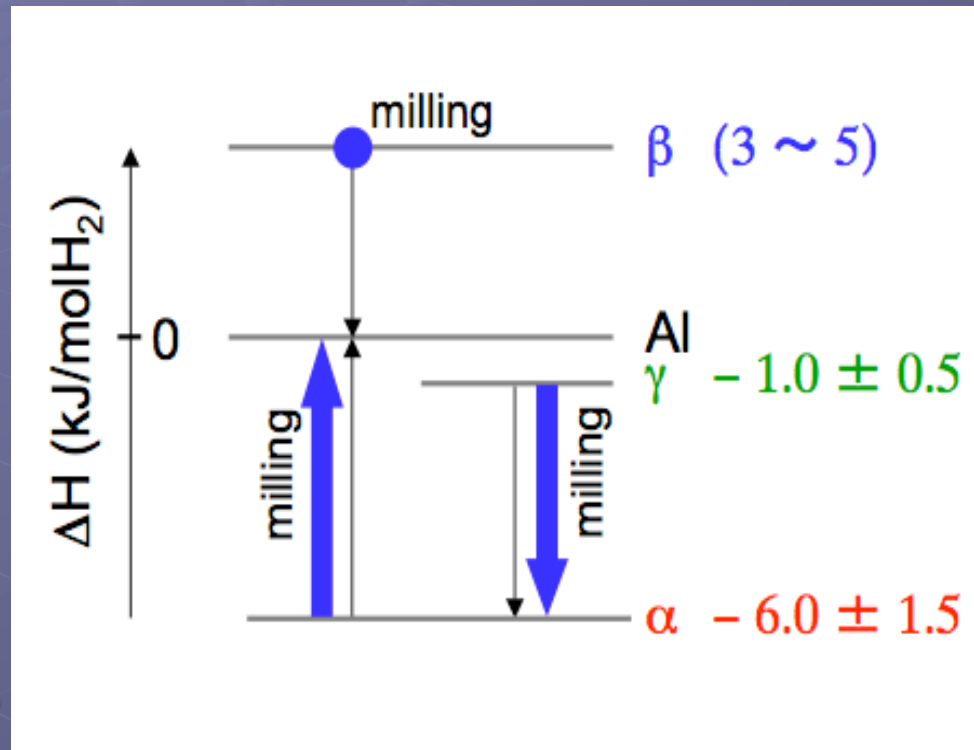
## TG-DTA



Thermogravimetry and differential thermal analysis of the three phases of  $\text{AlH}_3$  before and after mechanical milling.

S. Orimo, Y. Nakamori, T. Kato, C. Brown, C.M. Jensen Appl. Phys. **2006** 117, 27.

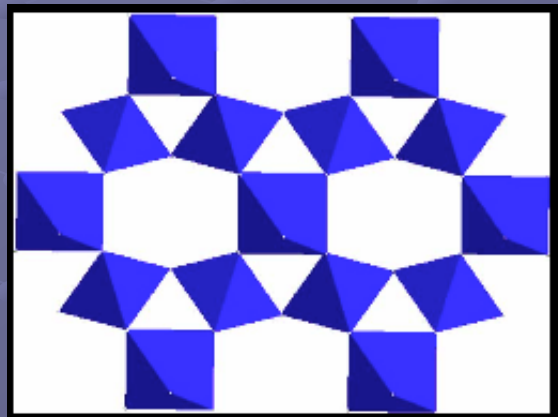
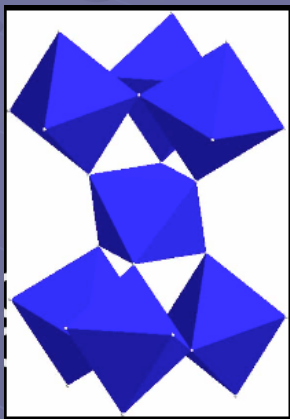
Enthalpies of dehydrating reactions  
 $\Delta H_{\text{dehyd.}}$  of the three phases of  $\text{AlH}_3$



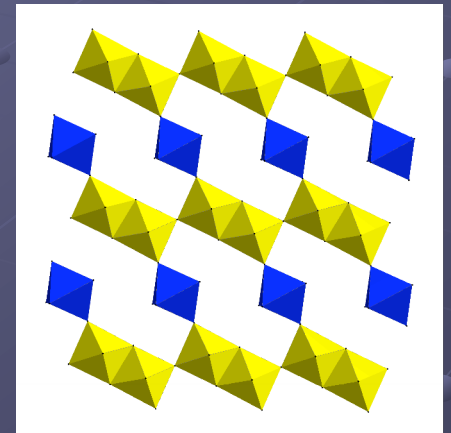
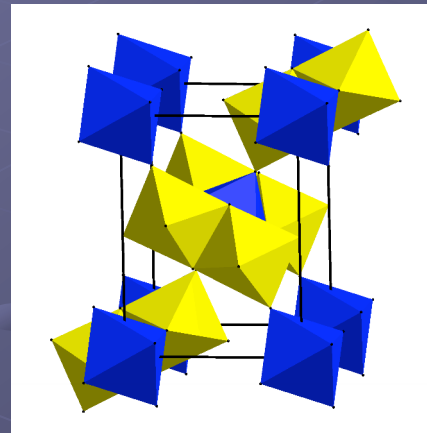
S. Orimo, Y. Nakamori, T. Kato, C. Brown, C.M. Jensen Appl. Phys.  
2006 117, 27.

# Neutron Structure Determination of $\beta$ and $\gamma$ phases of $\text{AlH}_3$

$\beta$   
phase



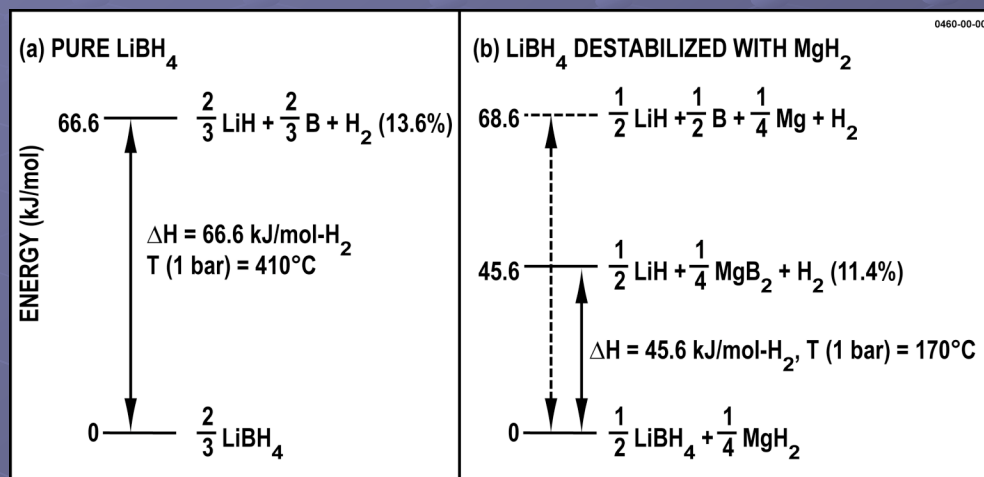
$\gamma$   
phase



H.W. Brinks, W. Langley, C.M. Jensen, J. Graetz, J.J. Reilly, B.C. Hauback, *J. Alloys Comp.* **2006** in press.

H.W. Brinks, C. Brown, C.M. Jensen, J. Graetz, J.J. Reilly, B.C. Hauback, *J. Alloys Comp.* **2006** in press.

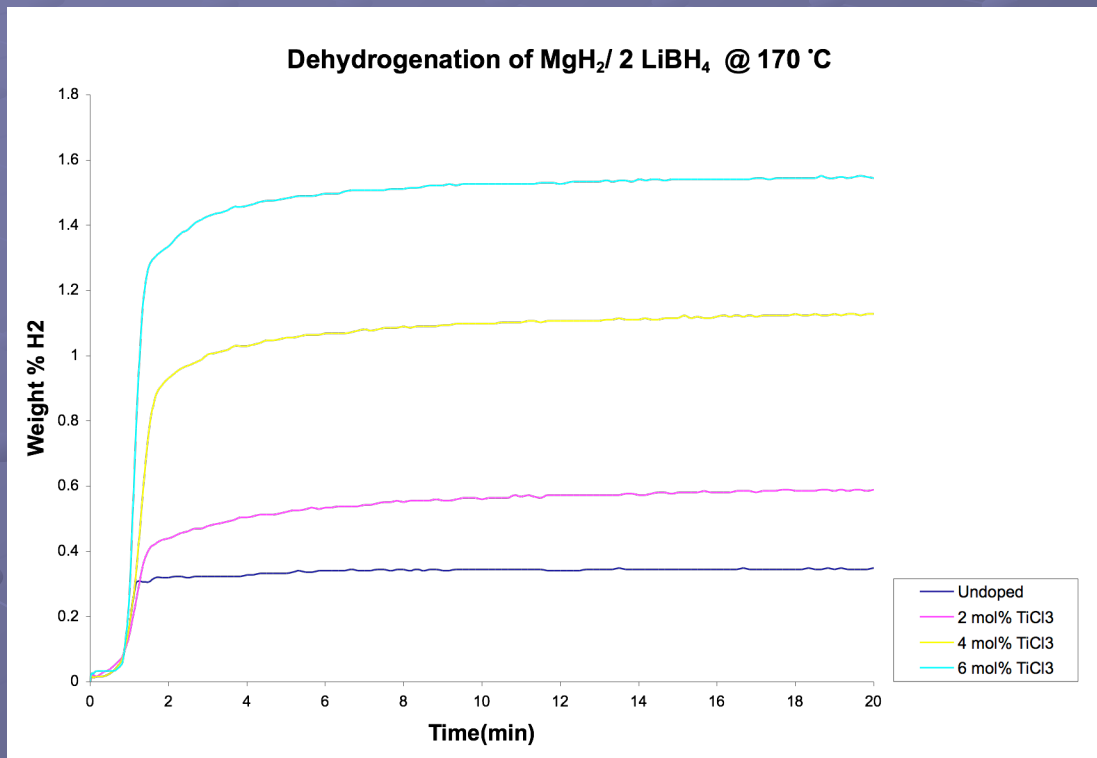
# Borohydride $[\text{BH}_4]^-$



- Formation of kinetic product,  $\text{MgB}_2$  prevents the formation of thermodynamic products, Mg and B.
- > 9 wt %  $\text{H}_2$  reversible.
- High kinetic barrier necessitates > 400 °C for rapid dehydrogenation.

J. Vajo, S. Skeith, F. Mertens *J. Chem. Phys* 2005, 109, 3719.

# Effects of Ti-dopants on the kinetics of the dehydrogenation of $\text{MgH}_2/2 \text{LiBH}_4$

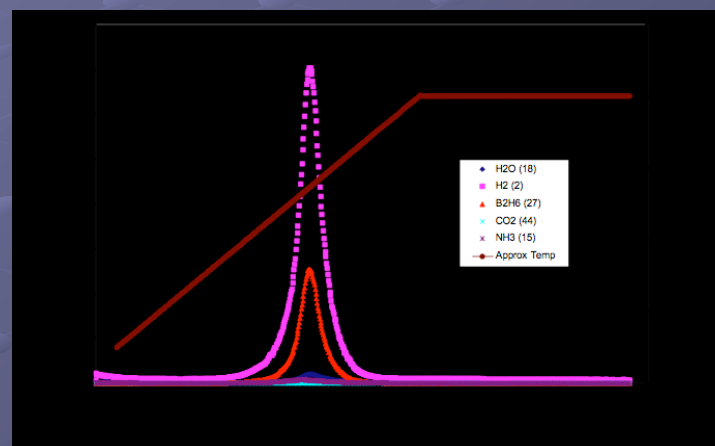
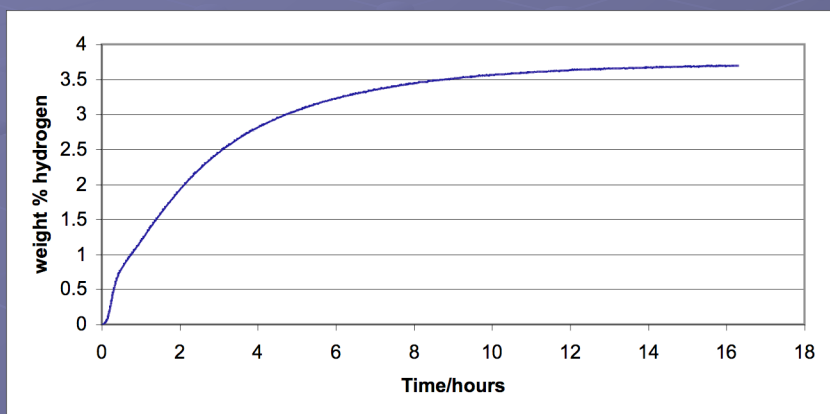


- $\text{TiCl}_3$  has a pronounced effect on the kinetics of the dehydrogenation of  $\text{MgH}_2/2 \text{LiBH}_4$ .
- No enhancement is observed during second cycle following rehydrogenation.
- Amount of rapidly released hydrogen has a linear relationship with amount of  $\text{TiCl}_3$  added.
- Similar effects have been found with upon addition of  $\text{TiCl}_3$  to  $\text{LiBH}_4$ .  
M. Au and A. Jurgensen *J Phys. Chem.* **2006**, *110*, 7062.

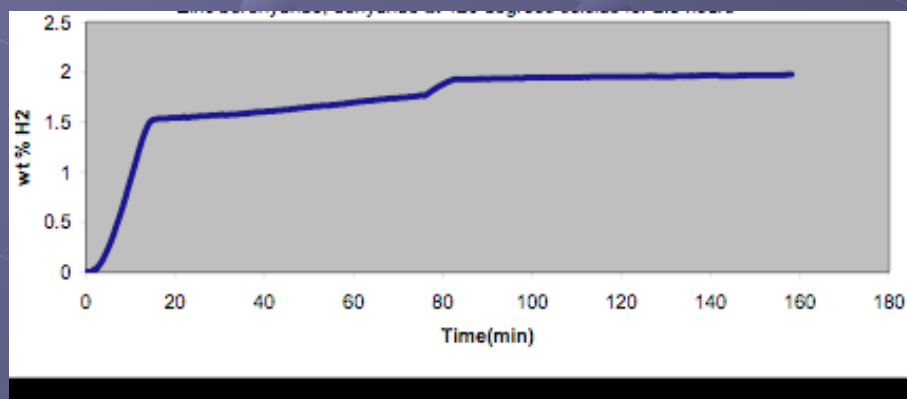
⇒ Kinetic effect is due to stoichiometric reaction between  $\text{LiBH}_4$  and  $\text{TiCl}_3$ .

# Production of Diborane Upon Dehydrogenation of Novel Borohydrides

## Dehydrogenation at 120 °C

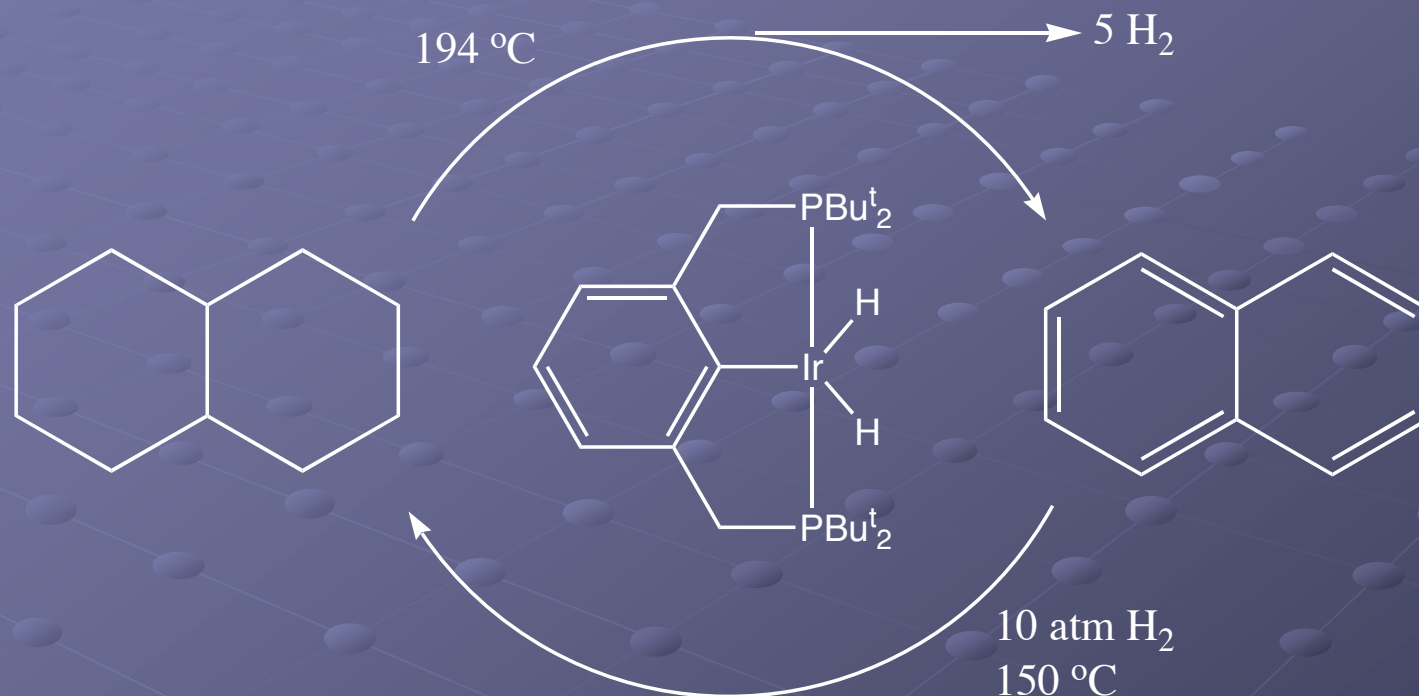


## Dehydrogenation at 100 °C



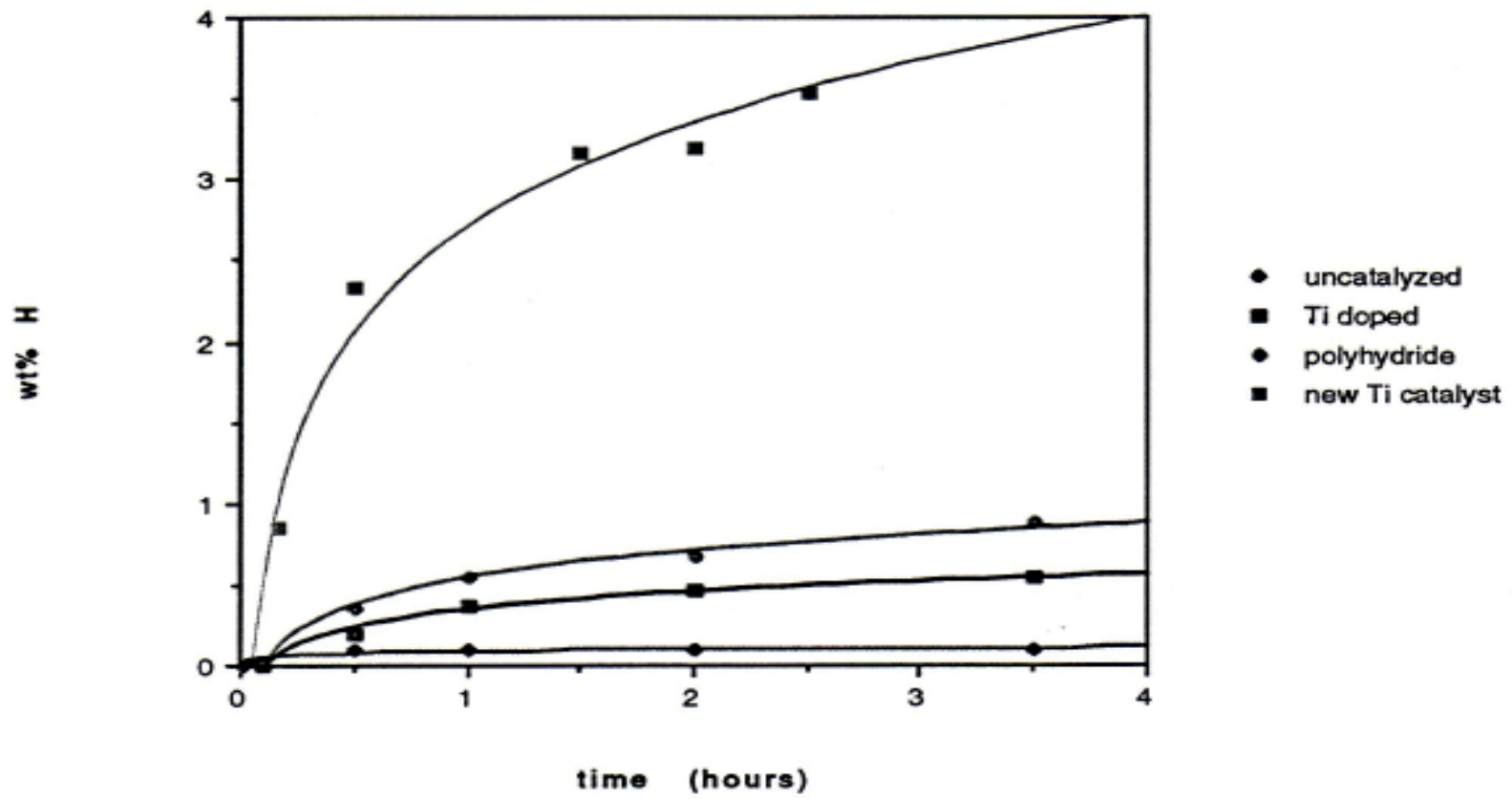
Dehydrogenation is Reversible IF second Step avoided

# Hydrogen Storage via Reversible Dehydrogenation of Cycloalkanes

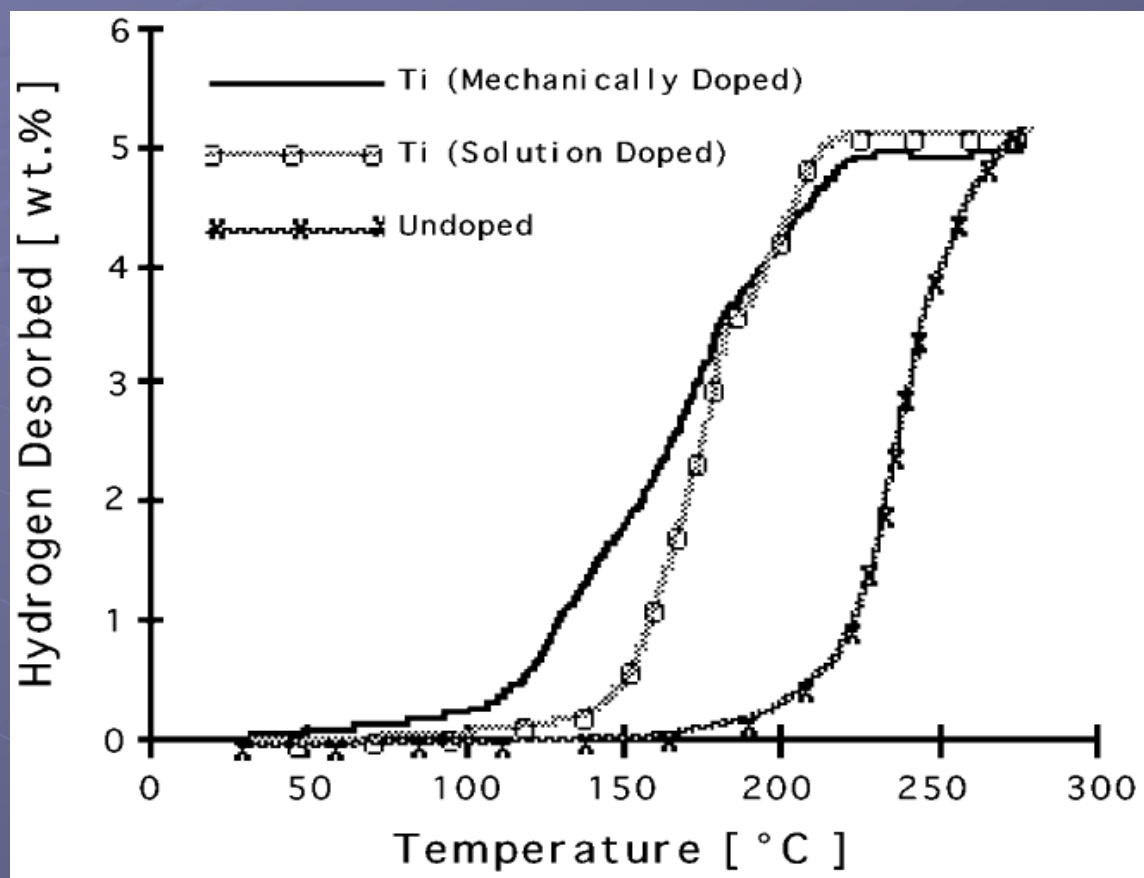


C.M. Jensen *Proceedings of the 1997 U.S. DOE Hydrogen Program Review* 307.  
C.M. Jensen US Patent 6,074,447 2000.

## Dehydrogenation of NaAlH<sub>4</sub> at 120 °C



# Mechanically Doped NaAlH<sub>4</sub>

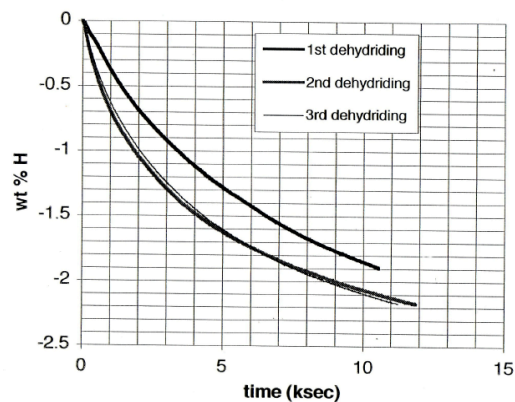


R.A. Zidan, S. Takara, A.G. Hee, and C.M. Jensen, *J. Alloys Compd.* **1999**, 285, 119.  
C.M. Jensen and R.A. Zidan, U.S. Patent 6,471,935 **2002**.

# Maximization of hydrogen cycling performance of Ti-doped NaAlH<sub>4</sub>

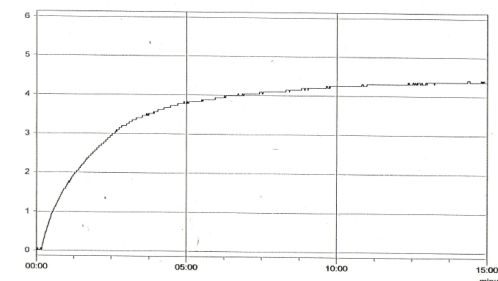
## Dehydrogenation:

Rate of 1.8 wt % per hour observed at 100 °C for 2 mol % Ti doped NaAlH<sub>4</sub> to Na<sub>3</sub>AlH<sub>6</sub> is adequate to meet the demands of an onboard PEM fuel cell.



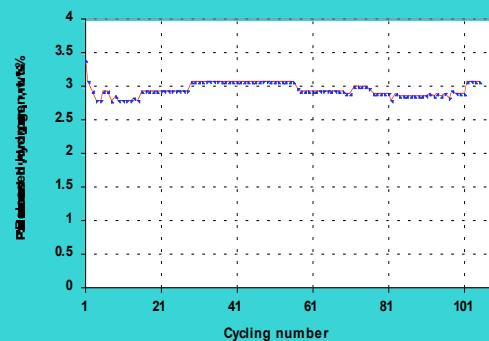
## Re-hydrogenation

Hydrogen Absorption by 2 mol % Zr Doped NaH + Al at 100 °C under 100 atm H<sub>2</sub>

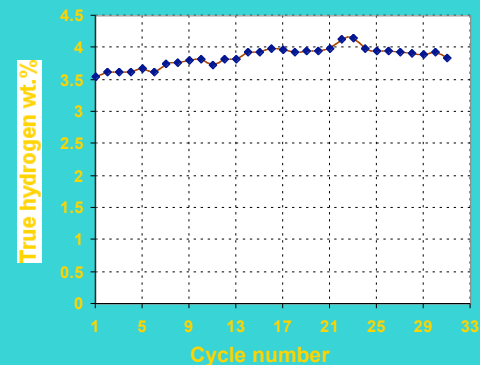


## Cycling Tests of 2 mol % Ti-doped Na/Al

Desorption: 120 °C, 3h. Absorption: 100 atm, 100 °C



Desorption: 150 °C, 3h. Absorption: 100 atm, 100 °C

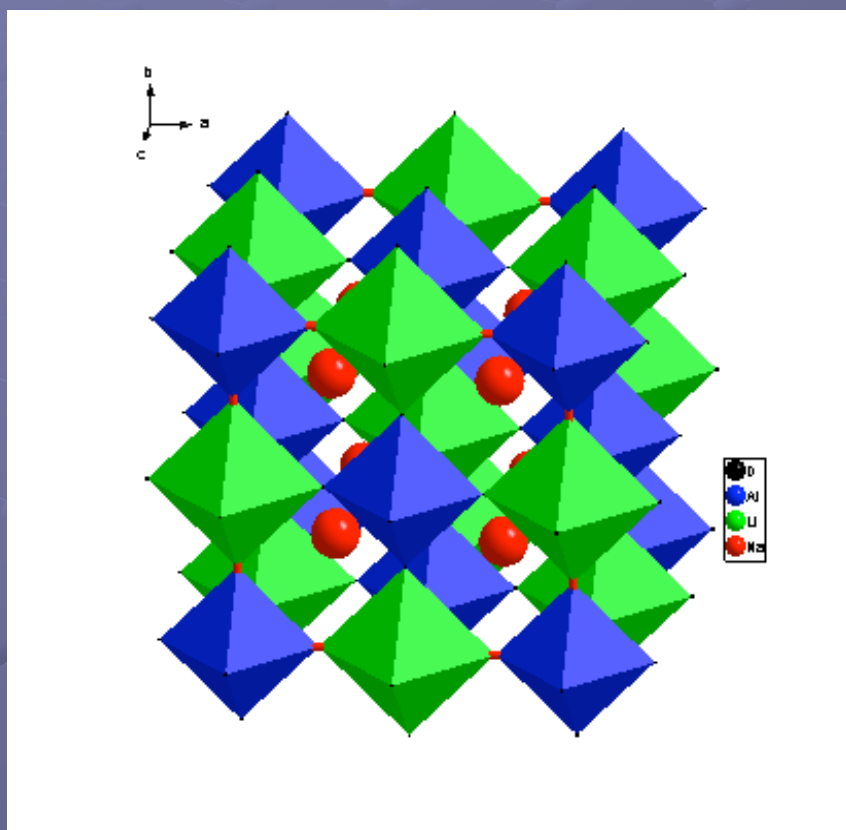


S.S. Srinivasan, H.W. Brinks, B.C. Hauback, D. Sun, C.M. Jensen, *J. Alloys Compd.* 2004, 377, 283.

# Barriers to Practicality

- Plateau Pressures of  $\text{Na}_3\text{AlH}_6$  /  $\text{NaH} + \text{Al}$  is too low.
- Rate of dehydrogenation of  $\text{Na}_3\text{AlH}_6$  to  $\text{NaH} + \text{Al}$  is too slow.
- Heat management during re-hydriding of practical scale hydride beds
- Cycling Capacity of 3.0 - 4.0 wt % is too low.
- Dehydrogenation of other alanates (ie.  $\text{LiAlH}_4$  and  $\text{Mg}(\text{AlH}_4)_2$  ) are irreversible under  $\text{H}_2$  pressure under moderate conditions.

# Neutron Diffraction Structure Determination of $\text{Na}_2\text{LiAlD}_6$



Ccp array of  $[\text{AlD}_6]^{3-}$  complex ions with Li filling the octahedral sites and Na filling the tetrahedral sites.

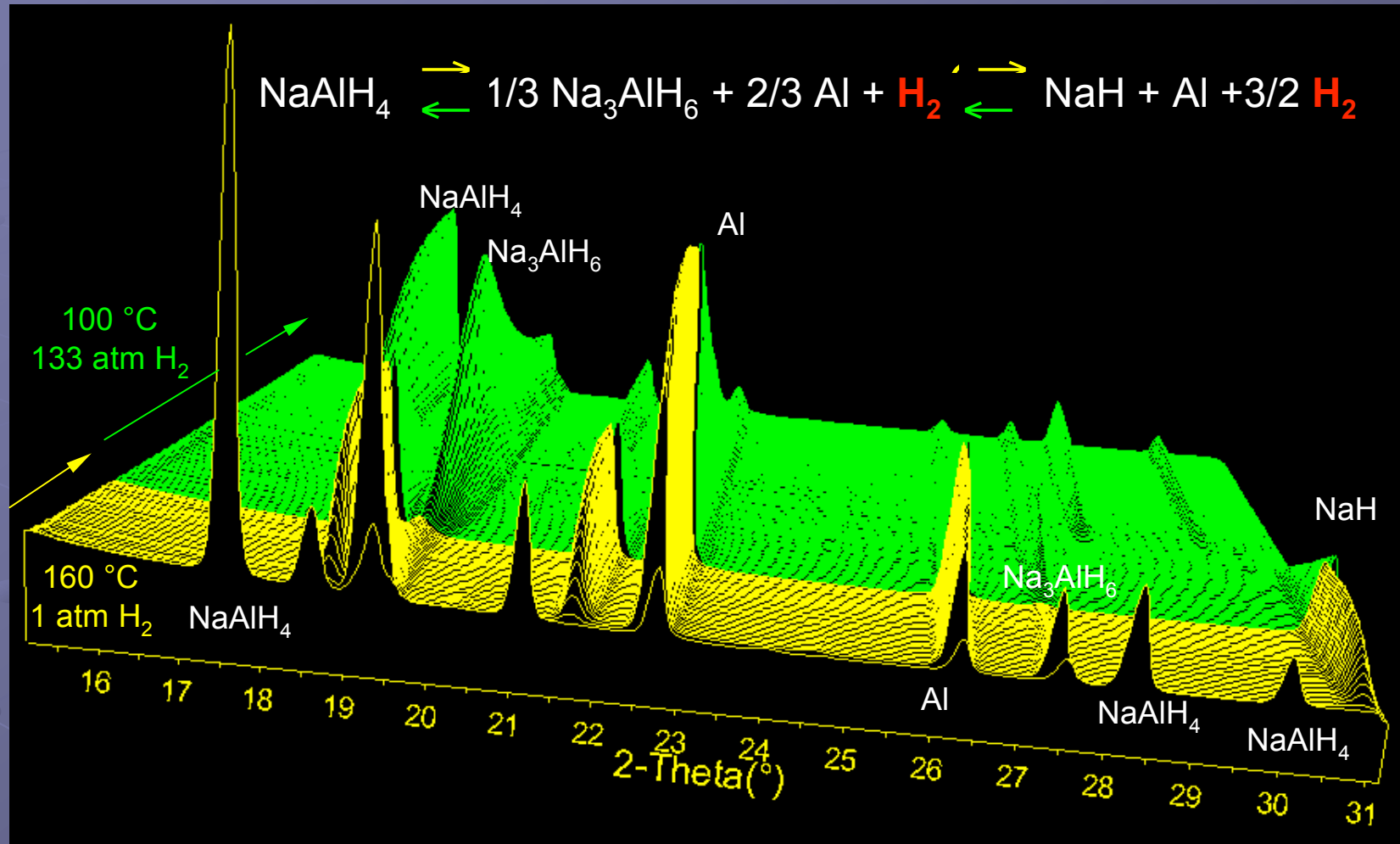
Selected inter-atomic distances (in Å) and angles (in  $^\circ$ ) for  $\text{Na}_2\text{LiAlD}_6$  at 295 K

Atoms	Distances
Al-D	1.760(3)
Li-D	1.933(3)
D-D	2.488(3), 2.734(3)
Al-Al	5.222
Na-Li	3.198
Na-Na	3.692
Li-Li	5.222
Atoms	Angles
D-Al-D	90.00(-), 180.00(-)

Estimated standard deviations in parentheses (for the inter-metallic distances the standard deviations are  $<0.0005$  Å).

H.W. Brinks, B.C. Hauback, C.M. Jensen, and R. Zidan; *J. Alloys and Compd.* 2005, 392, 27.

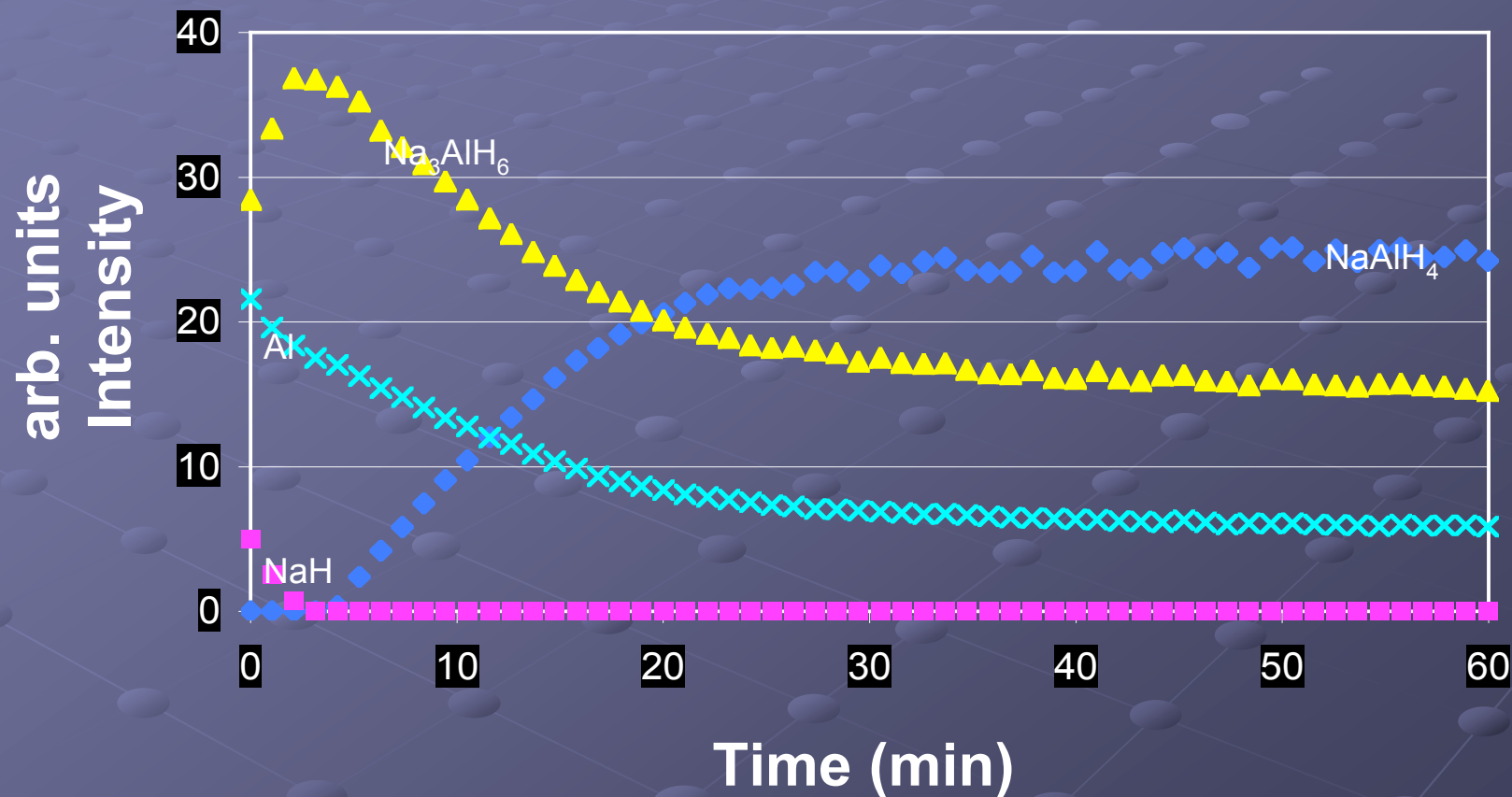
# In situ Synchrotron XRD



⇒ Stepwise pathway also followed for **rehydrogenation**

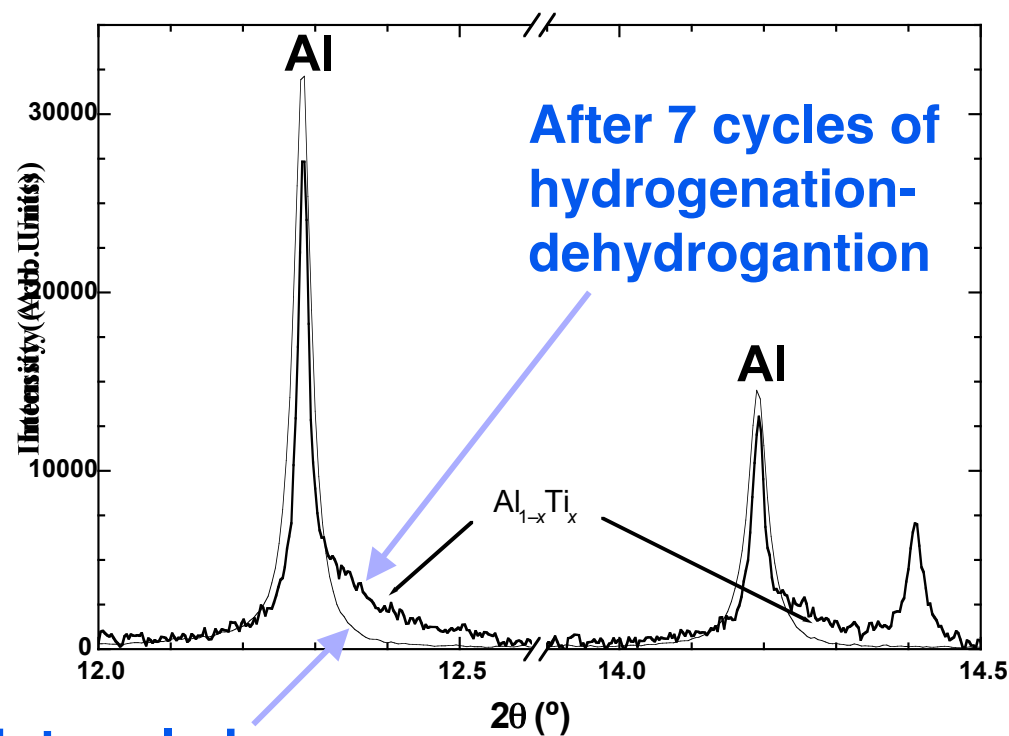
J. Rijsenbeek, Y. Gao, C.M. Jensen, and S. Srinivasan submitted for publication

# Cycling of NaAlH<sub>4</sub> doped with 2 mol % TiF<sub>3</sub>



J. Rijsenbeek, Y. Guo, S.S. Srinivasan, and C.M. Jensen, submitted for publication.

# Cycling introduces shoulders on the Al XRD peaks



Rietveld refinements indicate that the shoulders correspond to a solid solution of Ti in Al of composition  $\text{Al}_{0.93}\text{Ti}_{0.07}$ .

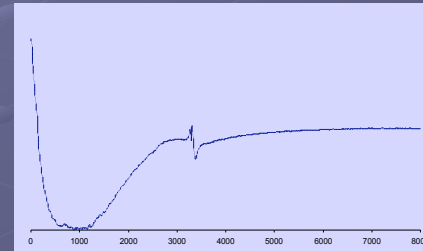
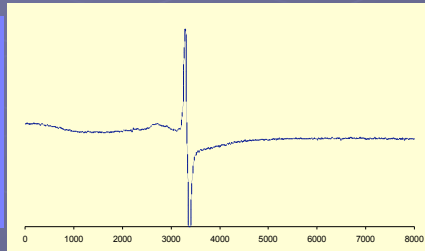
H.W. Brinks, C.M. Jensen, S.S. Srinivasan, B.C. Hauback, D. Blanchard, K. Murphy *J. Alloys Compd.* 2004, 376, 215.

# Electron Paramagnetic Resonance

Collaboration with Prof. Sandra Eaton,  
University of Denver

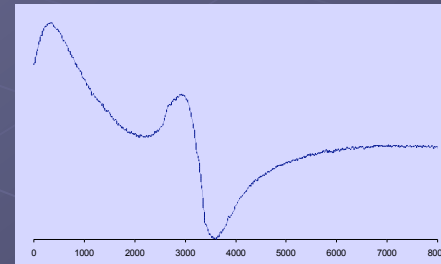
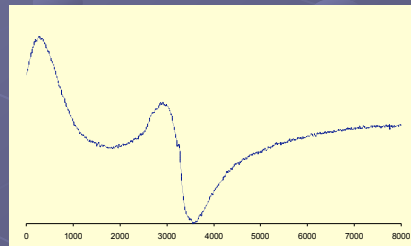
NaAlH<sub>4</sub> doped with 2.0 mol % of TiF<sub>3</sub>   NaAlH<sub>4</sub> doped with 2.0 mol % of TiCl<sub>3</sub>

Upon doping The spectrum of is dominated by sharp signal with  $g = 1.976$  and  $\Delta B_{pp} \sim 90$  G that is characteristic of spin isolated Ti(III).



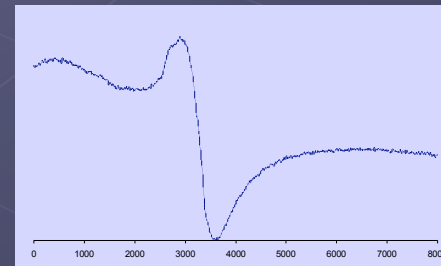
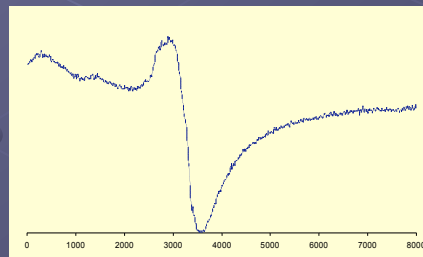
Upon doping. The spectrum is dominated by a strong signal near zero-field. There is also a small signal with  $g \sim 1.97$  that is quite similar to the Ti(III) signal that is observed in the TiF<sub>3</sub> doped sample.

After 5 cycles Instead of the signal with  $\Delta B_{pp} \sim 90$  G or  $\Delta B_{pp} \sim 1500$  G, the spectrum is dominated by a signal with  $\Delta B_{pp} \sim 650$  G. There is also a signal near zero-field.



5 Cycles. There is now a signal with  $g = 2.01$  and  $\Delta B_{pp} \sim 650$  G plus a signal near zero-field that is quite different from the original one. This spectrum is very similar to TiF<sub>3</sub> doped sample after 5 cycles.

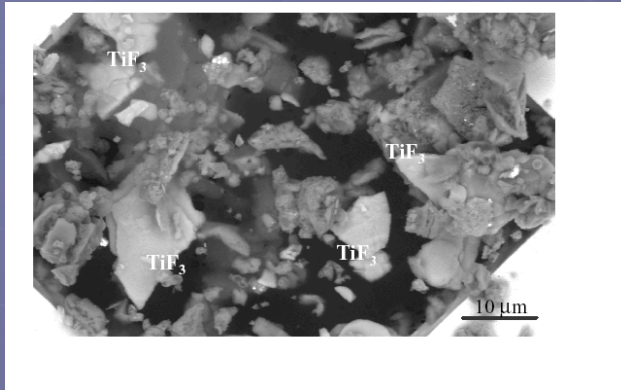
After 10 cycles Only the Ti(0) signal near zero-field has largely disappeared and only the Ti(0) signal at  $\Delta B_{pp} \sim 650$  G.



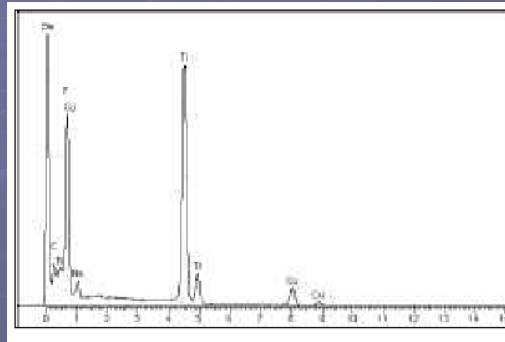
After 10cycles. Only the Ti(0) signal near zero-field has largely disappeared and only the Ti(0) signal at  $\Delta B_{pp} \sim 650$  G.

# Tunneling and Scanning Electron Microscopy

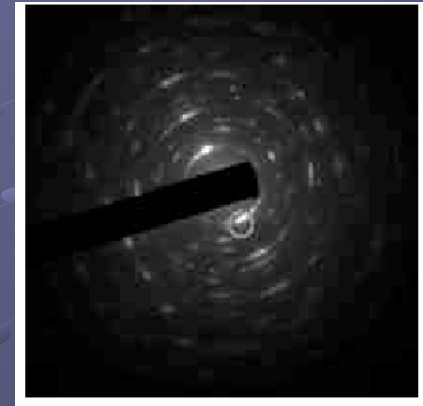
Collaboration with Dr. C. Andrei and Prof. R. Holmstad,  
Norwegian University of Science and Technology



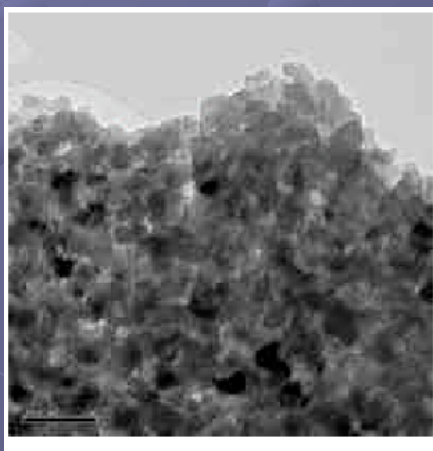
SEM image taken with backscattered electrons (BSE).



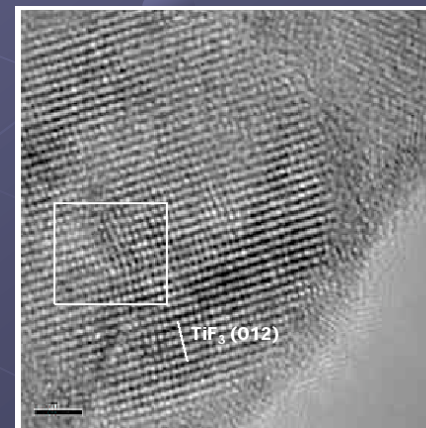
Energy Dispersive X-ray spectrum of a particle observed in uncycled  $NaAlH_4$  doped with 2 mol %  $TiF_3$  shows strong Ti and F peaks.



Small Angle Diffraction pattern of a Ti, F rich particle matches  $TiF_3$ .



TEM bright field image of a Ti, F rich particle observed in uncycled sample of  $NaAlH_4$  doped with 2 mol %  $TiF_3$ .

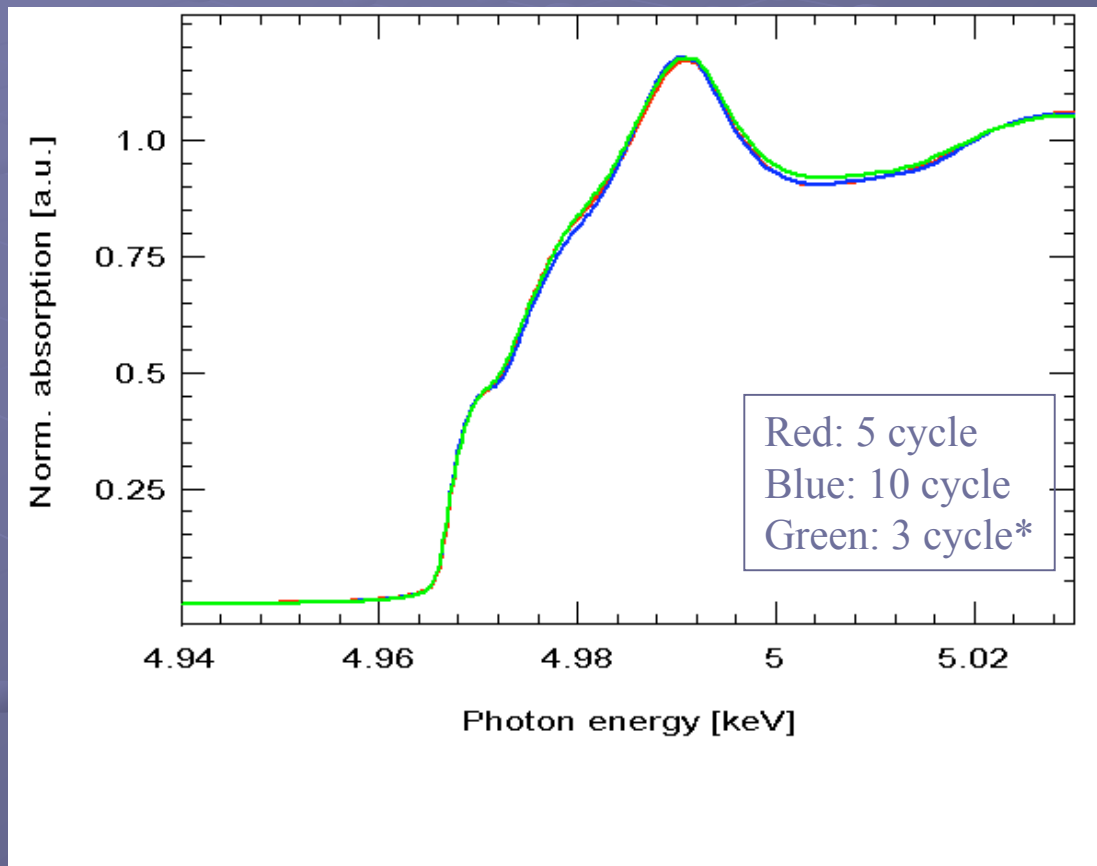


High resolution image of  $TiF_3$  grain. Indicated lattice planes were indexed as  $TiF_3$ .

- No correlation between Al and Ti seen in the EDS maps directly after ball milling but correlation, suggesting Al-Ti bonding, seen after 15 cycles.
- No significant change in grain size after 15 cycles

C.M. Andrei, J. Walmsley, H.W. Brinks, R. Holmestad, C.M. Jensen, B.C. Hauback *Appl. Phys. A.* **2005** 80, 709.

# X-ray Absorption Spectroscopy



Comparison of Ti K-edge XANES for samples doped with 2 mol %  $\text{TiF}_3$  and a 3 cycle sample doped with 2 mol %  $\text{TiCl}_3$  (green). These three samples have identical near-edge features, indicating the same Ti oxidation state.

J. Rijsenbeek, Y. Gao, C.M. Jensen, and S. Srinivasan submitted for publication

# X-ray Absorption Spectroscopy

“Al<sub>3</sub>Ti forms immediately on doping with TiCl<sub>3</sub> and oxidation state is nearly invariant during hydrogen cycling” - J. Graetz, J.J. Reily, J. Johnson, A.Y. Ingotov, T.A. Tyson *Appl. Phys. Lett.* **2004** 85, 500.

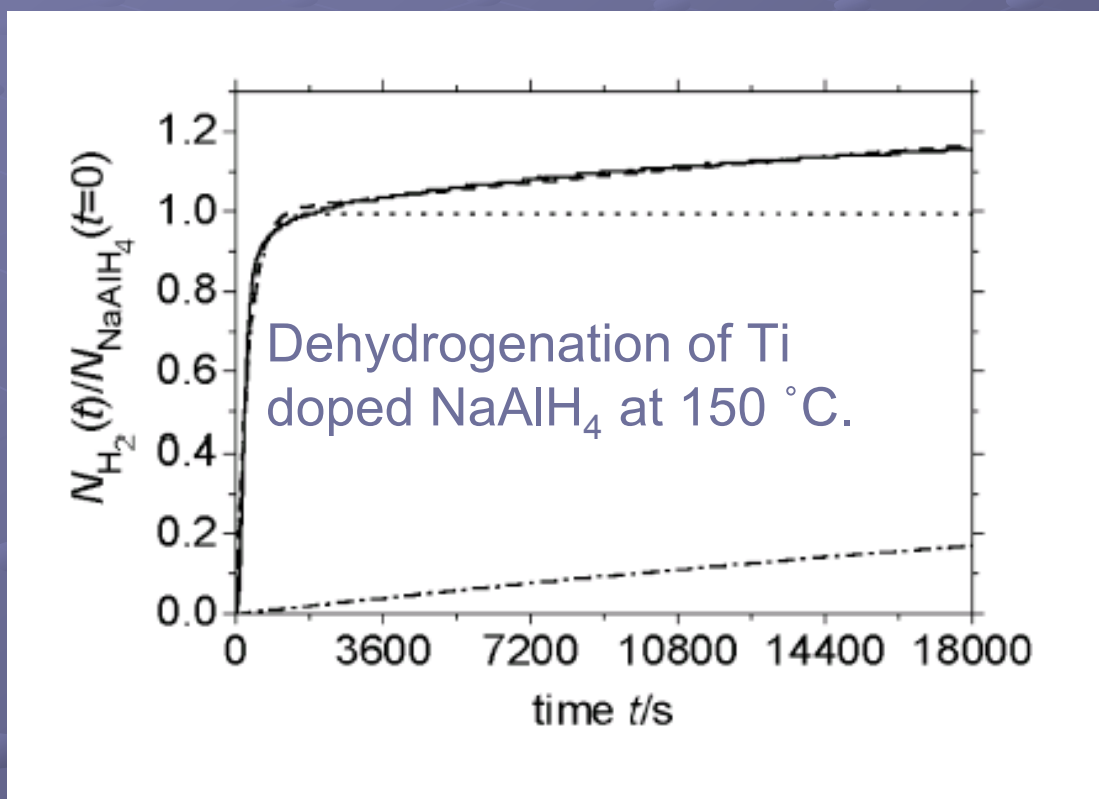
“Ti(0) species are formed immediately on doping and state is nearly invariant during hydrogen cycling with TiCl<sub>3</sub>. The formation of an alloy with Al or TiH<sub>2</sub> is **not** supported by EXAFS data.” - A. Leon, O. Kircher, J. Rothe, M. Fichtner, *J. Phys. Chem.* **2004** 16372.

Only a relative minor change in the hydrogen cycling kinetics occurs whether the majority of titanium is Ti(III) or Ti(0).

⇒ the enhanced hydrogen cycling kinetics are due to a Ti species that is present in only a relatively minor amount.

# Kinetic Studies: Elucidation of Rate Determining Step

Collaboration with Dr. T. Kiyobayashi, Institute for Advanced Science and Technology, Osaka Japan



- Dehydrogenation of Na<sub>3</sub>AlH<sub>6</sub> is much slower than NaAlH<sub>4</sub> starting with Ti-doped NaAlH<sub>4</sub>
- Dehydrogenation profiles can be closely simulated using rate constants determined from relative simple kinetic model

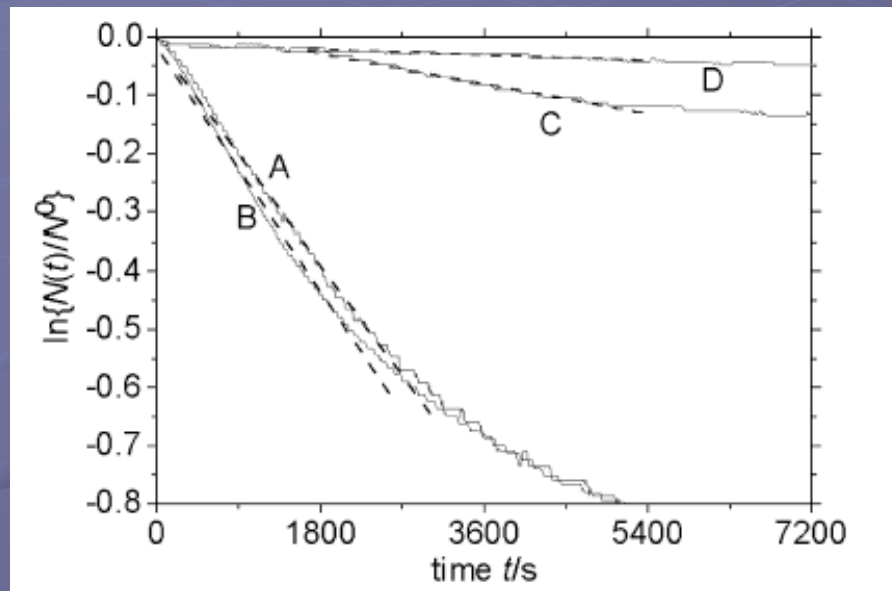
T. Kiyobayashi, S.S. Srinivasan, D. Sun, C.M. Jensen, *J. Phys. Chem. A* **2003**, *107*, 7671.

# Relation between $N_{\text{H}_2}(t)$ and the rate constants $k_1$ and $k_2$

$$\frac{N_{\text{H}_2}(t)}{N_{\text{NaAlH}_4}^0} = \left\{ 1 - \frac{k_2}{2(k_1 - k_2)} \right\} \{1 - \exp(-k_1 t)\} + \left\{ \frac{k_1}{2(k_1 - k_2)} \right\} \{1 - \exp(-k_2 t)\}$$

- Assumed the two reversible dehydrogenation are first order and independent.
- Rate equations are treated as simultaneous differential equations
- Best fits obtained for  $k_1 = 3.5 \times 10^{-3} \text{ s}^{-1}$  and  $k_2 = 2.3 \times 10^{-5} \text{ s}^{-1}$

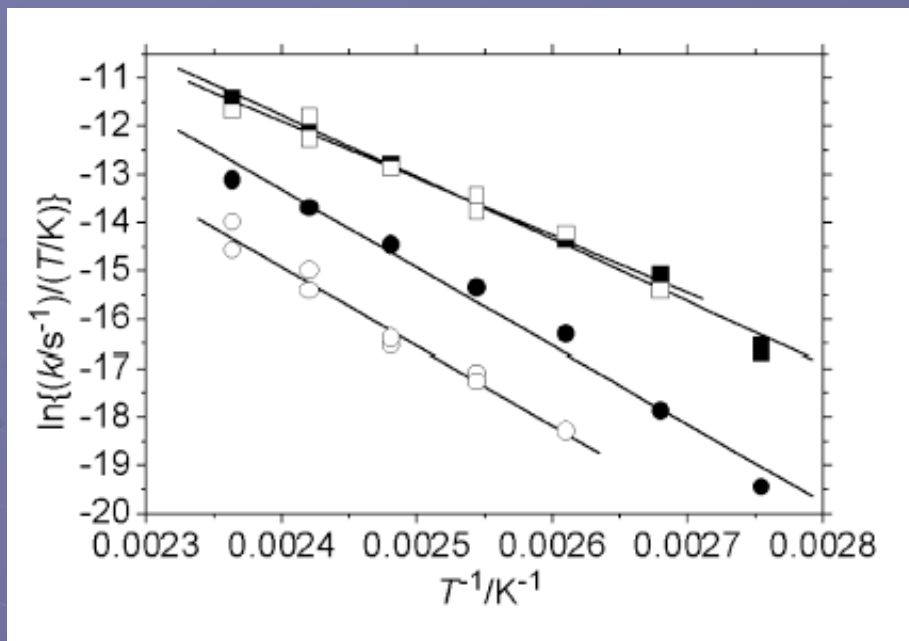
.....but directly Ti doped  $\text{Na}_3\text{AlH}_6$  undergoes dehydrogenation at rates equal to that of Ti doped  $\text{NaAlH}_4$ !!



Dehydrogenation profiles at 110 °C of:  
A) Ti-doped  $\text{NaAlH}_4$   
B) Ti-doped  $\text{Na}_3\text{AlH}_6$   
C) Zr doped  $\text{NaAlH}_4$   
D) Zr doped  $\text{Na}_3\text{AlH}_6$

Dehydrogenation kinetics are not controlled by relative strengths Al-H bonds.  $\Rightarrow$  Kinetics are limited by processes long range atomic transport phenomenon and location of dopants

T. Kiyobayashi, S.S. Srinivasan, D. Sun, C.M. Jensen, *J. Phys. Chem. A* **2003**, *107*, 7671.



Eyring plots of rates constants for the dehydrogenation of

A) Ti doped  $\text{NaAlH}_4$  ■

B) Ti doped  $\text{Na}_3\text{AlH}_6$  —

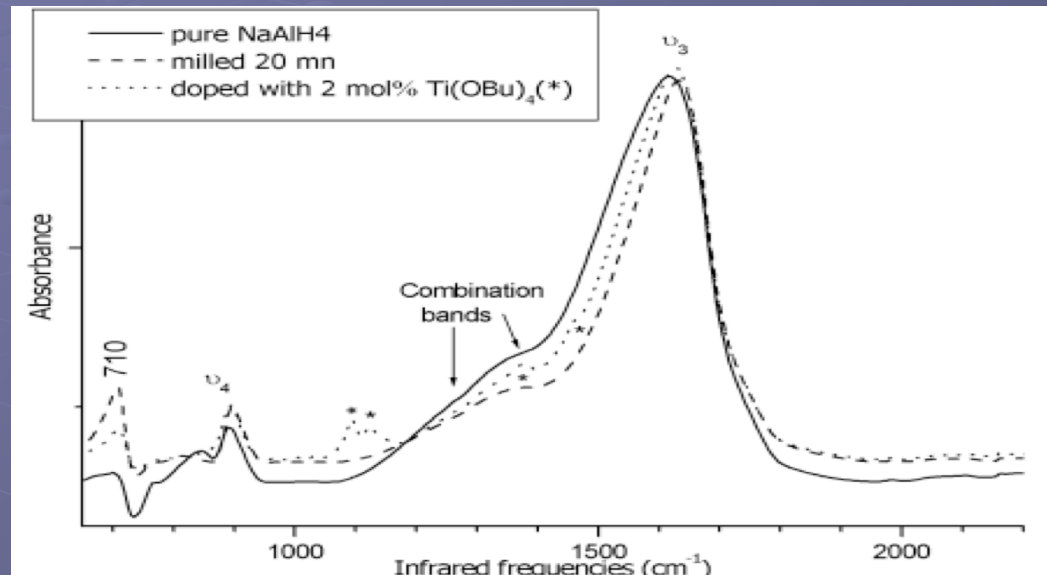
C) Zr doped  $\text{NaAlH}_4$  ●

D) Zr doped  $\text{Na}_3\text{AlH}_6$  ○

Enthalpies of activation,  $\Delta H$  (kJ/mol) of Ti and Zr doped  $\text{NaAlH}_4$  and  $\text{Na}_3\text{AlH}_6$

	Ti doped	Zr doped
$\text{NaAlH}_4$	$100 \pm 7$	$134 \pm 16$
$\text{Na}_3\text{AlH}_6$	$99 \pm 13$	$135 \pm 17$

# Infrared Spectroscopy

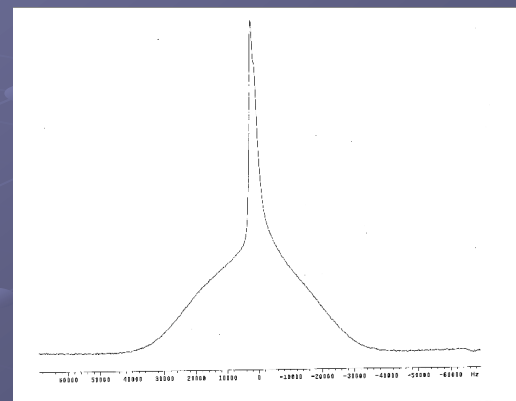


Al-H stretching frequency shifts  $\Rightarrow$  Al bonding is perturbed upon doping and/or ball milling.

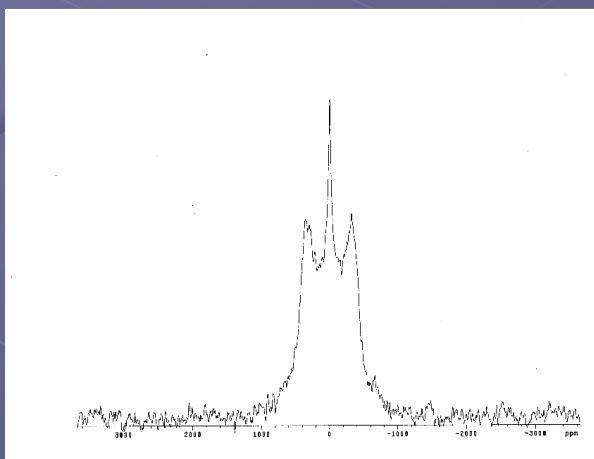
S. Gomes, G. Renaudin, H. Hagemann, K. Yvon, M.P. Sulic, and C.M. Jensen *J. Alloys Compds* **2005** 390, 305.

# $^1\text{H}$ and $^2\text{H}$ Nuclear Magnetic Resonance Spectroscopy

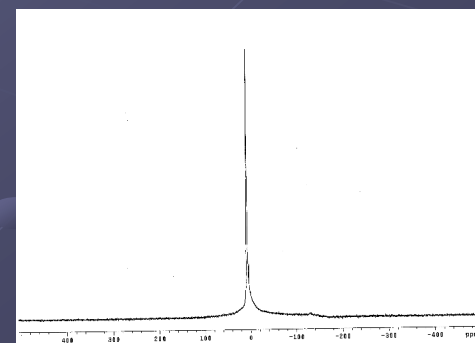
The  $^1\text{H}$  NMR spectrum of  $\text{NaAlH}_4$  consists of an expected broad component with a very long, 2000 sec,  $T_1$  relaxation time and an anomalous sharp component with a short, 240 ms relaxation time indicating that it corresponds to highly mobile population of hydrogen. The sharp component is often ascribed to residual solvent BUT.....



The  $^2\text{H}$  NMR spectrum of  $\text{NaAlD}_4$  that is prepared in protio-solvents also contains a sharp component.

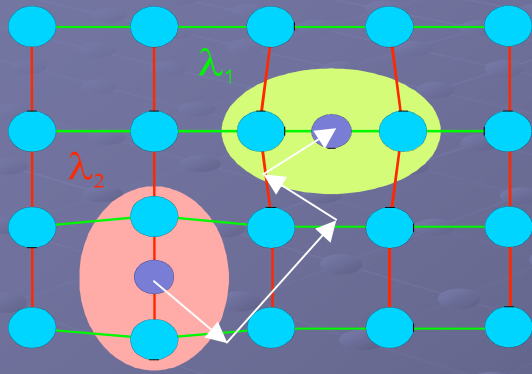


We have also eliminated the possibility that the sharp component is free  $\text{H}_2$  gas as its spectrum consists of a resonance that is much narrower and has a  $T_1$  of 13 msec.



# Anelastic Relaxation

Prof. R. Cantelli, University of Rome



Long range component of the strain due to defects  
Elastic dipoles  $\lambda$  (hopping with time  $\tau$ )

$$\text{Anelastic strain } \varepsilon^{\text{an}} = \lambda_1 n_1 + \lambda_2 n_2$$

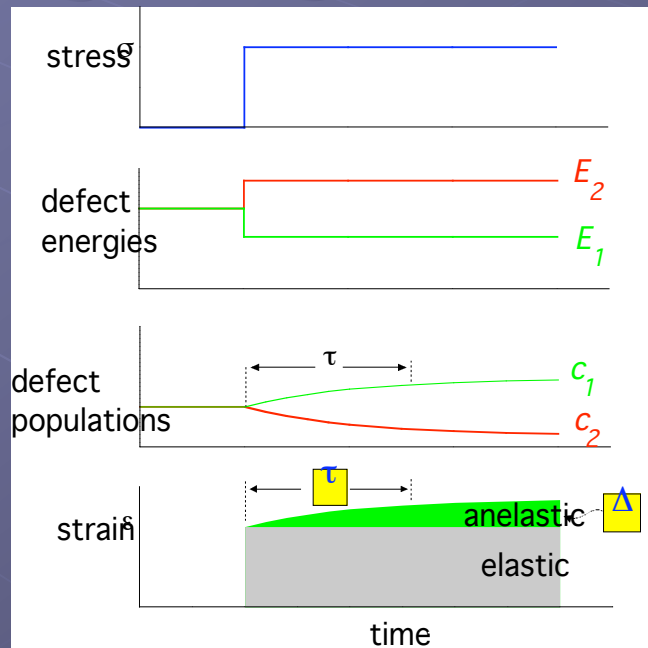
$$\text{Stress } \sigma: dE_i = -\lambda_i \sigma$$

Boltzmann distribution:

$$n_i = \exp(-E_i/kT)$$

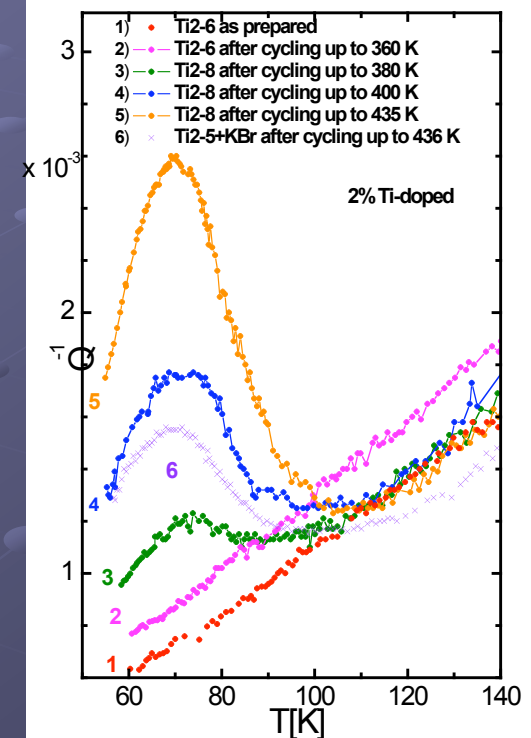
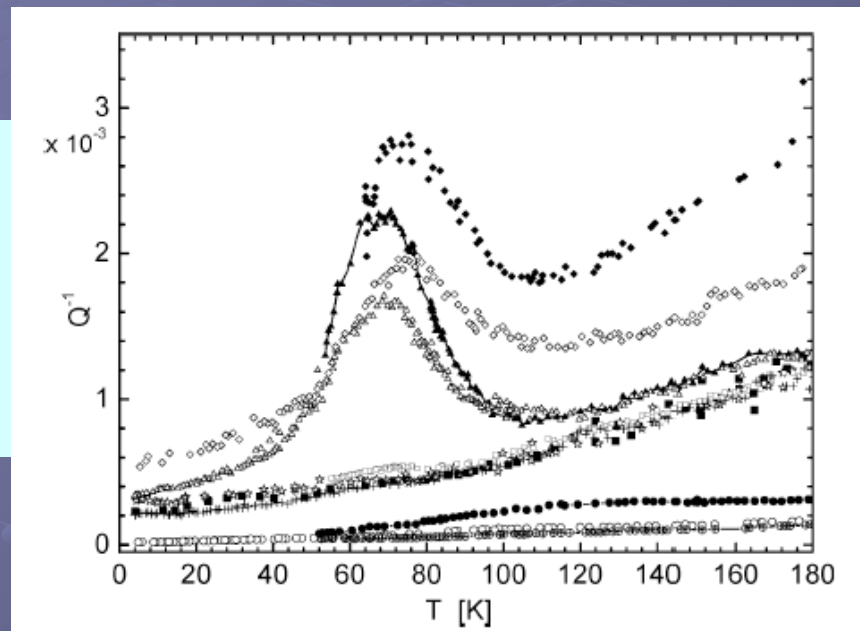
Relaxation strength:

$$D = e^{\text{an}}/e^{\text{el}} \sim (\Delta\lambda)^2/T$$



# Low Temperature Dependence of Elastic Energy Loss

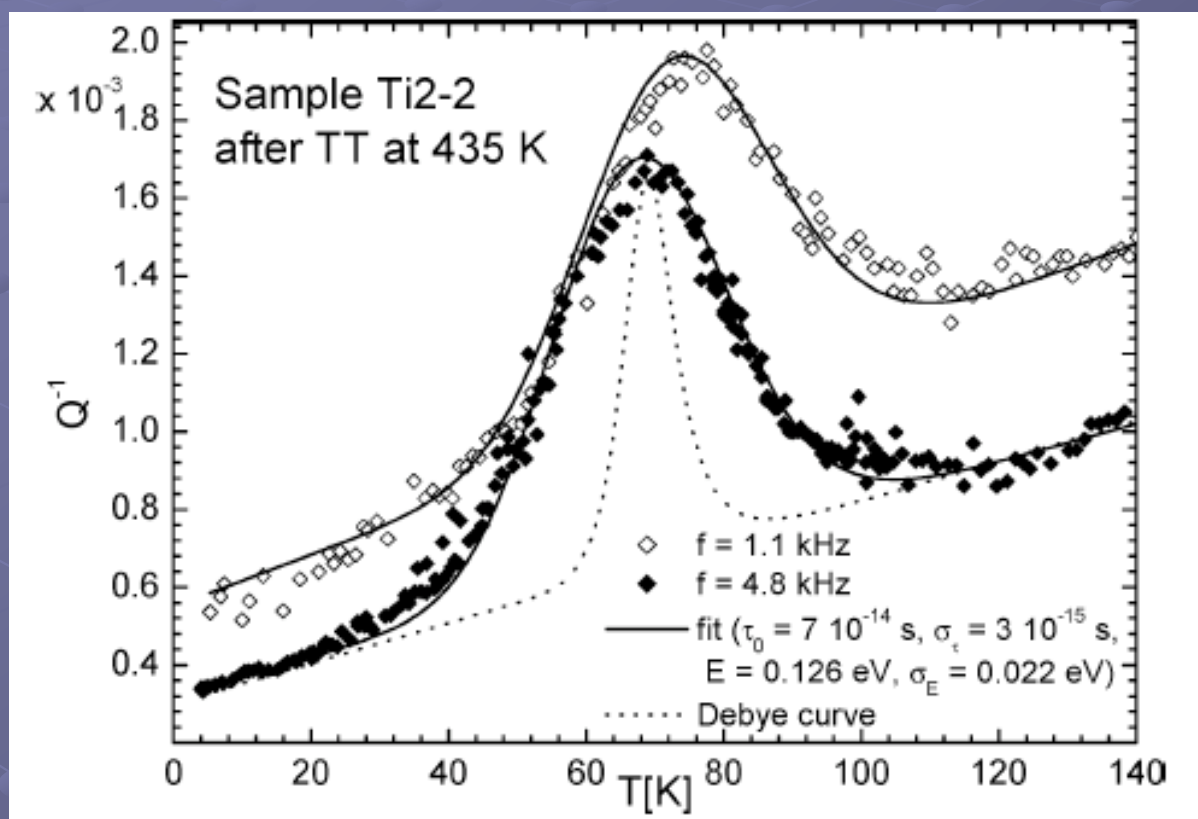
- KBr only
- KBr, H<sub>2</sub> treated
- undoped  
undoped, TT
- ▲ doped, TT, 1.1 Hz
- ◆ doped, TT, 4.8 Hz
- △ doped, TT, 1.1Hz, aged
- ◇ doped, TT, 4.8 Hz, aged



⇒ A point-defect is formed during the dehydrogenation of the Ti-doped hydride that gives rise to a thermally activated relaxation process.

O. Palumbo, R. Cantelli, A. Paolone, C.M. Jensen, S.S. Srinivasan *J. Phys. Chem. B.* **2005**, *109*, 1168.

# Experimental curve is much broader than predicted for a single Debye process



⇒ At 70 K, the relaxing entities (very likely hydrogen) are strongly interacting and/or highly mobile, performing about  **$5 \times 10^3$  jumps/s** (corresponding to an activation energy of **0.126 eV**).

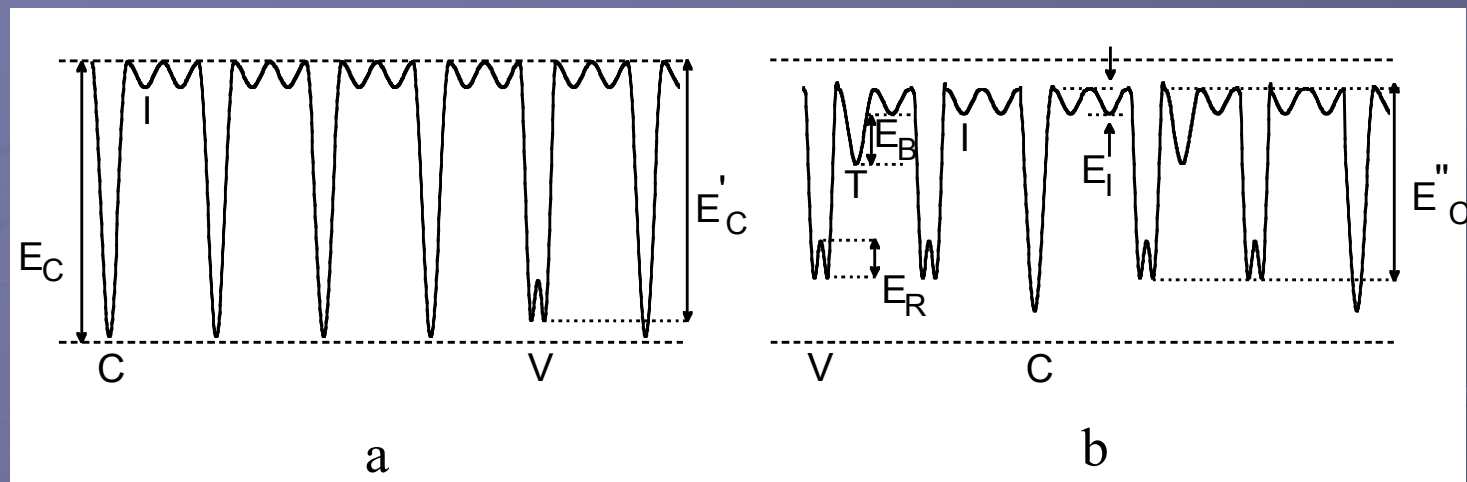
O. Palumbo, R. Cantelli, A. Paolone, C.M. Jensen, S.S. Srinivasan *J. Phys. Chem. B.* 2005, 109, 1168.

Anelastic spectroscopy has provided insight into the mechanism of the reversible dehydrogenation of Ti-doped  $\text{NaAlH}_4$ .

Observation of a deuterium isotope effect in the low temperature spectra shows that a mobilized population of hydrogen (defect hydride complexes) plays a fundamental role in the reversible dehydrogenation of  $\text{NaAlH}_4$ .

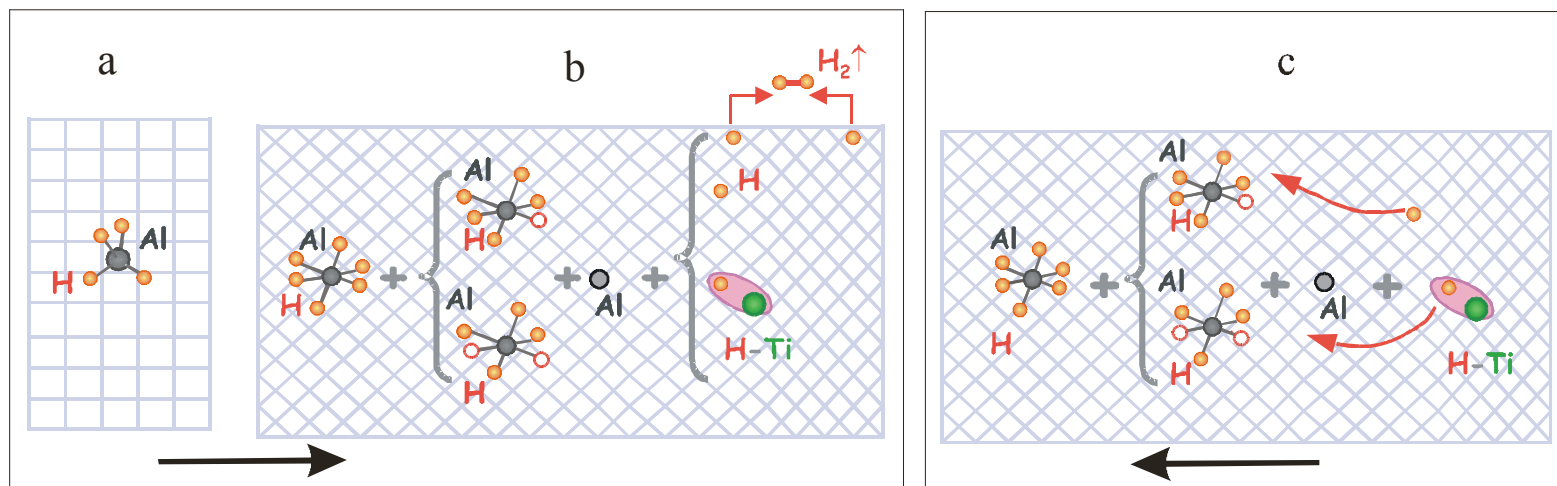
The formation of defect complex anions in concert with the formation of  $\text{Na}_3\text{AlH}_6$  and takes place at much lower temperatures upon Ti doping of the hydride.

⇒ Ti atoms decrease the energy barrier to breaking the Al-H bonds.



Schematic representation of the proposed potential energy of H atoms in thermally treated  $\text{NaAlH}_4$ : (a) undoped and (b) Ti-doped. Minima correspond to: chemical bond sites (labelled as C), lattice sites coordinated with the titanium trap (T), interstitial sites (I), and vacancy sites (V).  $E_R$  is the activation energy for vacancy relaxation (reorientation) and  $E_C$ ,  $E'_C$ ,  $E''_C$  are the energies for H to break the bonds.  $E_I$  is the activation energy for H interstitial migration,  $E_B$  the binding energy of H to Ti.

O. Palumbo, A. Paolone, R. Cantelli, C. M. Jensen, and M. Sulic *J. Phys. Chem. B* **2006**, *110*, 9105.



Schematic representation of the proposed dehydrogenation model: a)  $\text{AlH}_4$  group of initial  $\text{NaAlH}_4$ ; b) products of thermal decomposition: formation of both  $\text{AlH}_6$  and  $\text{AlH}_x$  ( $x < 6$ ) units, segregated Al, interstitial H in free and Ti trapping sites. The H atoms migrating to the surface recombine as molecules and evolve as gas. c) H migration to the deepest trap (chemical bond) during a subsequent thermal treatment in which the decomposition reaction does not proceed significantly, and allows partial equilibrium to be reached.

O. Palumbo, A. Paolone, R. Cantelli, C. M. Jensen, and M. Sulic *J. Phys. Chem. B* **2006**, *110*, 9105.

# Conclusions

- Alane is a very promising candidate for practical onboard hydrogen storage BUT a viable method for recharging must be developed.
- Borohydrides are promising candidates for practical onboard hydrogen storage but kinetic barriers to dehydrogenation and side reactions leading to the elimination of diborane must be overcome.

# Conclusions

- EPR, synchrotron XRD, XAFS, and TEM studies indicate that for  $\text{NaAlH}_4$  doped with 2 mol %  $\text{TiF}_3$ , the majority population of Ti changes from a Ti(III) species ( $\text{TiF}_3$ ) to a Ti(0) species ( $\text{Al}_3\text{Ti}$ ) during the first few cycles dehydrogenation-rehydrogenation.
- Only a relative minor change in the hydrogen cycling kinetics occurs whether the majority of titanium is Ti(III) or Ti(0).  $\Rightarrow$  the enhanced hydrogen cycling kinetics are due to a Ti species that is present in only a relatively minor amount.
- Infrared spectra show that mechanical milling with or doping perturbs Al-H bonding.

# Conclusions

- Ti dopants can enhance the kinetics of the dehydrogenation  $\text{Na}_3\text{AlH}_6$  to rates similar to those that have been observed for Ti-doped  $\text{NaAlH}_4$  suggesting that positioning of Ti rather than Al-H bond strengths limit dehydrogenation kinetics.
- Anelastic spectroscopy has detected highly mobile point-defects in heat treated Ti-doped hydride  $\text{NaAlH}_4$  that involve hydrogen.

# Acknowledgements

U.S. Department of Energy Hydrogen Program

Ministry of Economy, Trade, and Industry of Japan (METI) NEDO project WE-NET

## Jensen Group

Reyna Ayabe

Celeb Brown

Lance Calnane

Todd Dalton

Dr. Chrystel Hagen

Allan Hee

Walker Langley

Brad Lewandowski

Meredith Kuba

Dr. Christine Morales

Keeley Murphy

Dr. Anne Richards

Aditya “Ashi” Savara

Godwin Severa

Thomas Seidl

Dr. Sesha “Raman” Srinivasan

Martin Sulic

Dr. Dalin Sun

Dr. Satoshi Takara

Dr. Ping Wang

## Collaborators

Dr. Ragaiy Zidan - Savannah River National Laboratory

Dr. Steven Guthrie, Dr. George Thomas, Dr. Karl Gross, Dr. Eric Majzoub - Sandia National Laboratory

Prof. Sandra Eaton - University of Denver

Dr. Tetsu Kiyobayashi, Dr. Nobuhiro Kuriyama, Dr. Hiroyoyuki Takeshita - National Institute for Advanced Industrial Science and Technology, Osaka, Japan

Dr. Kristin Kumashiro, Dr. Walter Niemczura - University of Hawaii

Dr. Hendrik Brinks, Prof. Bjorn Hauback, Dr. Arnulf Maeland - Institute for Energy Technology, Kjeller, Norway

Dr. Terry Udovic, Dr. Jorge Inguez, Tander Yildirim - National Institute of Standards and Technology

Prof. Klaus Yvon, Dr. Hans Hagemann, G. Renaudin, Sandrine Gomes - Université de Genève

Prof. Alberto Albinati - Università di Milano

Dr. Job Rijssenbeek, Dr. Yan Gao, G.E. Global Research Center

Prof. Rosario Cantelli, Oriele Palumbo, Annalisa Paolone - Università di Roma

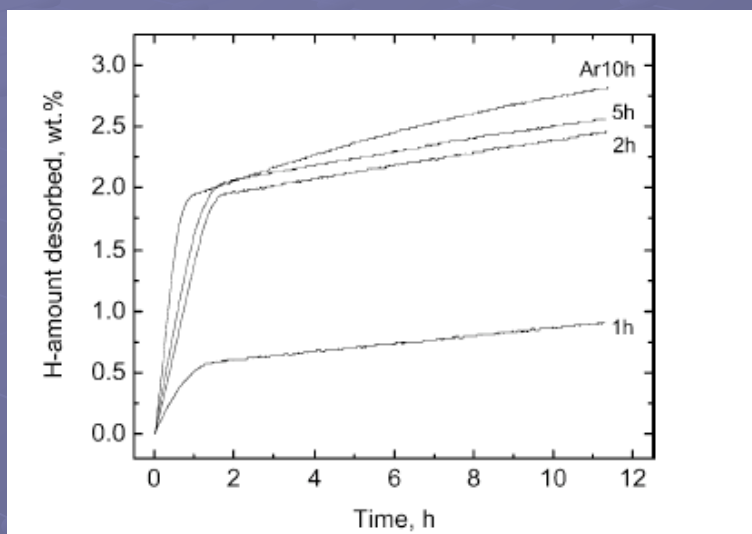
Dr. Carmen Andrei, J. Walmsley, R. Holmestad - Norwegian University of Science and Technology

## Spiritual Guidance

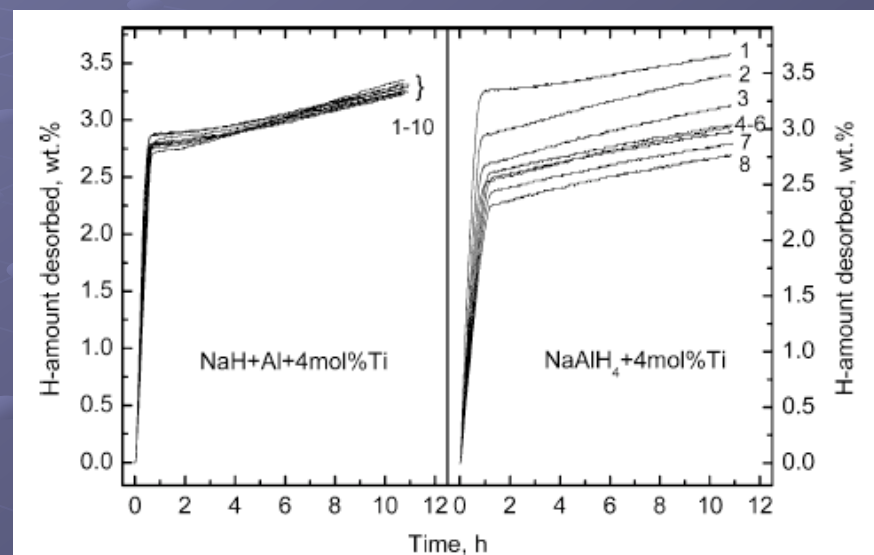
Dr. Gary Sandrock - Suna Tech



# Doping with Off-the-Shelf Ti Powder



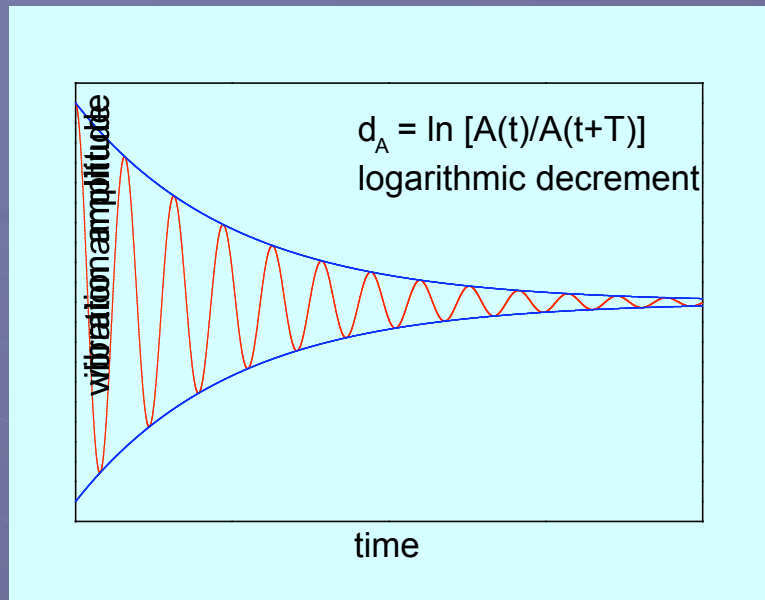
First dehydrogenation profiles at 150 °C for samples of NaH/Al + 4 mol % Ti powder mechanically milled for different periods



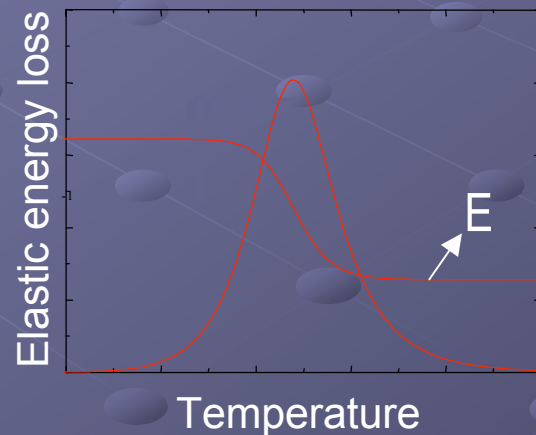
Comparison of the dehydrogenation Profiles of NaH/Al + 4 mol % Ti powder and NaAlH<sub>4</sub> + 4 mol % Ti both mechanically milled for 10h.

P. Wang and C.M. Jensen *J. Phys. Chem. B* 2004, 107, 14157.

# Relaxation process



- Elastic energy dissipation coeff.:  $Q^{-1} = M''/M'$  from the decay of the vibration amplitude or from width of resonance curve.
- The maximum of the elastic energy loss occurs when the angular vibration frequency is equal to the relaxation rate of the mobile species.



$$Q^{-1} = \frac{Mv_0(\lambda_1 - \lambda_2)^2 n_1 n_2}{T} \frac{1}{(\omega\tau)^\alpha + (\omega\tau)^{-\alpha}}$$